

Analyzing the potential for solar thermal energy utilization in the Chilean copper mining industry

Gonzalo Quiñones^a, Carlos Felbol^{a,*}, Carlos Valenzuela^a, Jose M. Cardemil^b, Rodrigo A. Escobar^{a,c}

^a Escuela de Ingeniería, Pontificia Universidad Católica de Chile, Av. Vicuña Mackenna 4860, Santiago, Chile

^b Departamento de Ingeniería Mecánica, Facultad de Ciencias Físicas y Matemáticas, Universidad de Chile, Av. Beauchef 851, Santiago, Chile

^c Centro del Desierto de Atacama, Pontificia Universidad Católica de Chile, Av. Vicuña Mackenna 4860, Santiago, Chile

ARTICLE INFO

Keywords:

Solar thermal energy
Industrial process
Parabolic trough
Flat plate collector
Evacuated tube collector
TRNSYS

ABSTRACT

Copper mining is the largest industry and energy consumer in Chile, utilizing heat from imported fossil fuels of which Chile is not a producer. The goals for decarbonization present opportunities to analyze how the Chilean industry can become sustainable with significant shares of renewable energy including solar heat. The present study analyzes the integration of solar heating to the copper refining process in order to gain insights on the technical, economical, and emissions performance of solar heating systems for the largest copper mining operations in Chile. The solar technologies considered in the analysis are flat plate, evacuated tube, and parabolic trough collectors. The results are validated by comparing with publicly available data from existing solar heating plants in copper mining facilities showing that solar plants are able to supply partially the thermal energy demand, although at different costs in terms of capital and operation and maintenance requirements. The economic analysis indicates that with current fossil fuel prices, solar heating technologies are a valid alternative for cost and emissions reduction in copper mining. Flat plate collectors show the lowest cost for solar heat when compared to evacuated tube and parabolic trough systems considering identical sets of technical and financial parameters. The parametric and sensitivity analysis indicate that the conditions under which solar heating is competitive with traditional fossil-fired heaters, which might still be required as backup systems in order to provide heat in a 24/7 regime, and in all the cases analyzed, a substantial reduction in CO₂ emissions can be achieved.

1. Introduction

Chilean energy matrix is mostly based on conventional sources to satisfy the electricity demand. As of 2018, 53.9% of the total installed power generation capacity corresponds to conventional fossil fuels thermal plants, 27.6% to hydro and 18.5% to non-conventional renewable energy sources (Asociación de Generadoras de Chile, 2018). A large share of the fossil fuels consumed is imported every year, e.g., in 2017, Chile imported 92% of its fossil fuel requirement, equivalent to 9.4 billion dollars each year (Comision Nacional de Energía, 2018; SNA, 2018). Approximately 32.7% of the fuels in Chile are used for generating heat in industrial processes (Comision Nacional de Energía, 2018). As a result, the country presents a big challenge exploring new alternatives that allow diversifying and reducing its energy dependence on imported fuels, as well as to satisfy carbon emission reduction goals.

In December 2015, Chile signed the Paris Agreement, compromising to reduce the greenhouse gas emissions between 30 and 45% per gross

domestic product (GDP) by 2030. Besides that, the Chilean Ministry of Energy released, in 2017, the Energy Policy 2050, which is a compendium of proposed actions focused on reducing by 30% the greenhouse gas emissions based on a 70% of renewable electricity generation (Ministry of Energy, 2017). In that context, the Solar Committee was created with the main objective of promoting the development of national solar industry and increasing the competitiveness, productivity, and capacities in the national solar market, taking advantage of the high solar resource in northern Chile (Comité Solar e Innovación Energética, 2019). As of 2019, the Chilean Government has announced a new plan for decarbonizing the economy, with the stated goals of close eight thermoelectric plants based in carbon in the next 5 years, which represent 19% of the total carbon-based plants capacity installed, and the total retirement of electricity generation plants based in carbon for 2040 (Gobierno de Chile, 2019).

Fig. 1 shows the energy consumption in Chile, where it is clearly depicted the industrial sector as the main energy consumer in the

* Corresponding author.

E-mail address: cjfelbol@uc.cl (C. Felbol).

<https://doi.org/10.1016/j.solener.2020.01.009>

Received 10 October 2019; Received in revised form 2 January 2020; Accepted 4 January 2020

Available online 11 January 2020

0038-092X/ © 2020 International Solar Energy Society. Published by Elsevier Ltd. All rights reserved.

Nomenclature

COCHILCO	Chilean Copper Commission
CNE	National Energy Commission
CSP	Concentrating Solar Power
DHI	Diffuse Horizontal Irradiation
DNI	Direct Normal Irradiation
ENIA	Annual National Industrial Survey
ER	Electrorefining
ETC	Evacuated Tube Collector
EW	Electrowinning
FIA	Agricultural Innovation Fund
FPC	Flat Plate Collector
O&M	Operation & Maintenance

CAPEX	Capital expenditures
GDP	Gross Domestic Product
OPEX	Operational expenditures
GHG	Greenhouse gas
GHI	Global Horizontal Irradiation
GWP	Global Warming Potential
IRR	Internal Rate of Return
LCOH	Levelized Cost of Heat
NPV	Net Present Value
PTC	Parabolic Trough Collector
SNA	National Customs Service
TMY	Typical Meteorological Year
TRNSYS	Transient System Simulation Program

country, demanding 128 TWh per year (which is 40% of the total yearly energy consumption of 322 TWh). More than half of energy consumption is used for process heat generation, in which fossil fuels play a significant role in satisfying the industrial demand, especially oil. The mining, paper & wood, and food industries concentrate most of the consumption of fossil fuels, where almost 67% of the energy is consumed in processes that operate at temperatures below 250 °C (Fundación Chile, 2015; Kalogirou, 2003).

Mining is the largest industry in Chile, responsible for 10% of 2018 GDP (Banco Central de Chile, 2018), and also the largest energy consumer in the country. For this reason, the mining sector constitutes a driver for Chilean development, but in turn, it is also one of the most polluting industries in the country (Ministerio del Medio Ambiente, 2018). The principal product of the Chilean mining industry is copper, for which the country is the world's largest exporter, accounting for 27.7% of the market share worldwide (Cochilco, 2018). Mining activities are mainly localized in Chilean central and northern regions. Regarding the energy demands in copper processing, one of the highest oil-consuming processes is the water heating for the solvent extraction and electrowinning (SX-EW) process. EW is the last process in the copper recovery system, just before the cathode harvesting. The process involves an aqueous solution called electrolyte that contains copper, sulfuric acid, and water, flowing inside of an array of cells, where an electrical potential is applied between anodes and cathodes, resulting in

the deposition of pure metallic copper from the electrolyte onto the cathodes. The process needs the electrolytic water-acid-copper solution to be kept at a temperature between 45 and 60 °C (Schlesinger et al., 2011). To warm the electrolyte, water heaters driven by oil are commonly used to deliver the heat load. Depending on the design of the plant and the heater integration scheme, the operational temperatures of the water after passing through the heaters are usually set between 60 and 90 °C (Kalogirou, 2003).

Fig. 2 shows the analysis from data published for Annual National Industrial Survey (ENIA) 2014, the national energy balance for Chile from 2015 and the annual report from Chilean mining council for 2015 (Consejo Minero, 2015; INE, 2014; Ministry of Energy, 2016), in this figure are presented different productive activities separated by industry, and the size of every section represents the size of the energy consumption associated to each activity. In this analysis, it is clearly shown that the copper mining industry is the largest fuel consumer for heat generation in Chile, reaching 21.2 TWh of energy consumption per year. The industry of paper, cellulose and wood is the second-largest heat consumer in its processes, reaching 20.6 TWh per year, but in this case, this industry generates its own heat from discarded biomass. In addition, it is worth to mention that the food industry represents the sixth part of the energy consumption for heat generation, with high potential for integrating solar technologies, since its processes commonly demand temperatures below 120 °C.

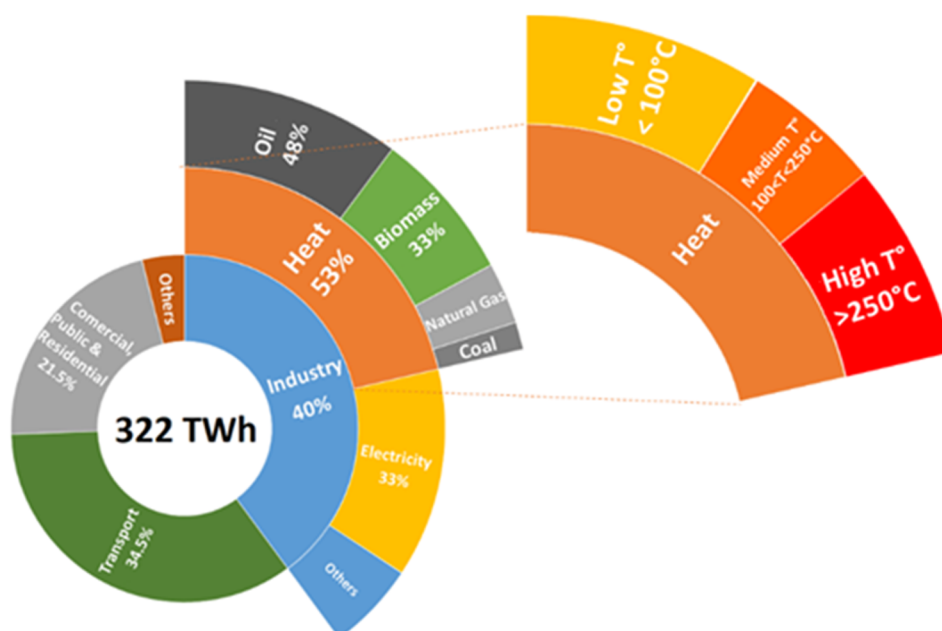


Fig. 1. Distribution of energy consumption in Chile in 2015 by sector (Cochilco, 2016; Ministry of Energy, 2016).

1.- Copper, 2.- Various mines, 3.- Lithium and Saltpeter, 4.- Paper and cellulose, 5.- Wood pulp, paper and cardboard, 6.- Other articles of paper and cardboard, 7.- Paper and cardboard containers, 8.- Sawing and planing, 9.- Fish, crustaceans and mollusks, 10.- Dairy products, 11.- Food products, 12.- Preparation and preservation of fruits, legumes and vegetables, 13.- Others, 14.- Meats, 15.- Bakery, 16.- Sugar and starches, 17.- Animal foods, 18.- Tobacco, 19.- Wines, 20.- Others, 21.- Concrete, cement and plaster articles, 22.- Iron and steel industry, 23.- Metallic products for structural use, 24.- Others, 25.- Fertilizers and nitrogen compounds, 26.- Others, 27.- Other industries, 28.- Other reparations, 29.- Machinery repair, 30.- Agricultural and forestry machinery, 31.- Electronic equipment repair, 32.- Others.

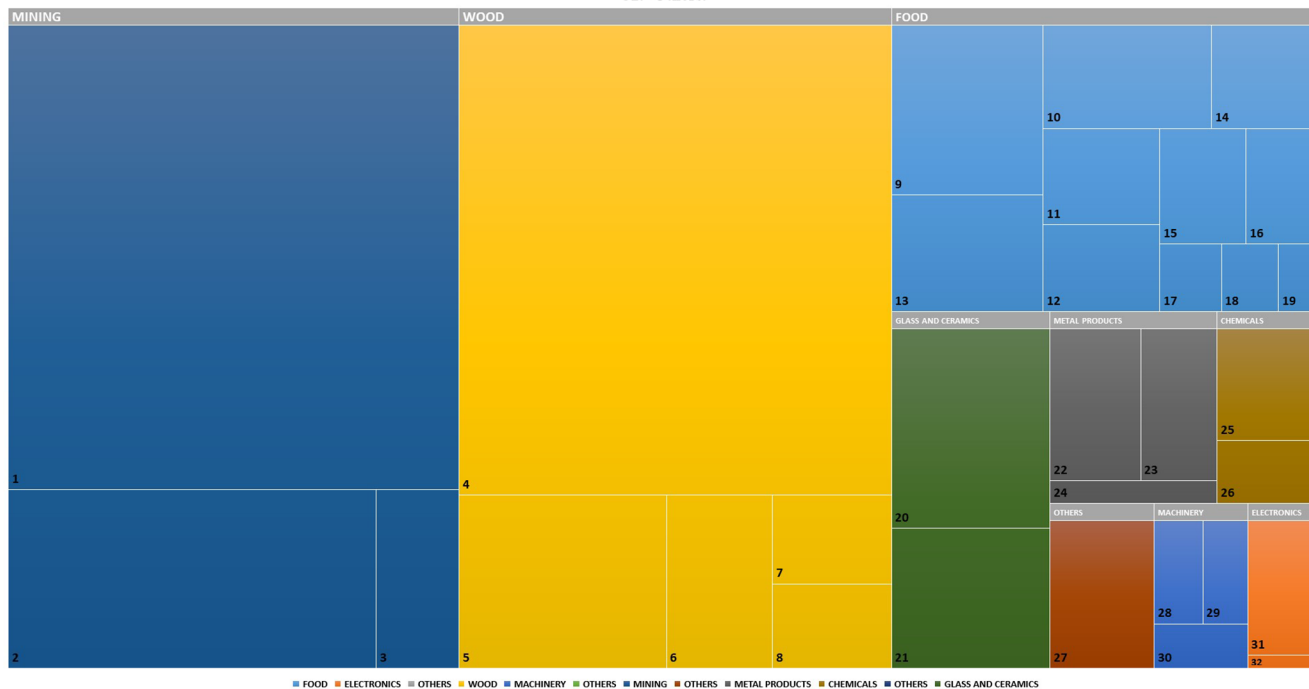


Fig. 2. Energy consumption for heat generation in industrial processes: Industrial and mining sector.

Although Chile offers excellent conditions for implementing solar energy solutions for process heat integration to mining operations, there is not yet a clear tendency towards the adoption of these technologies mostly, due to the existence of many different entry barriers,

such as an immature market for solar thermal solutions, insufficient local products, a lack of trained human capital and social awareness are present in context of all solar technologies, also there are economical and financial barriers which include volatile energy prices and

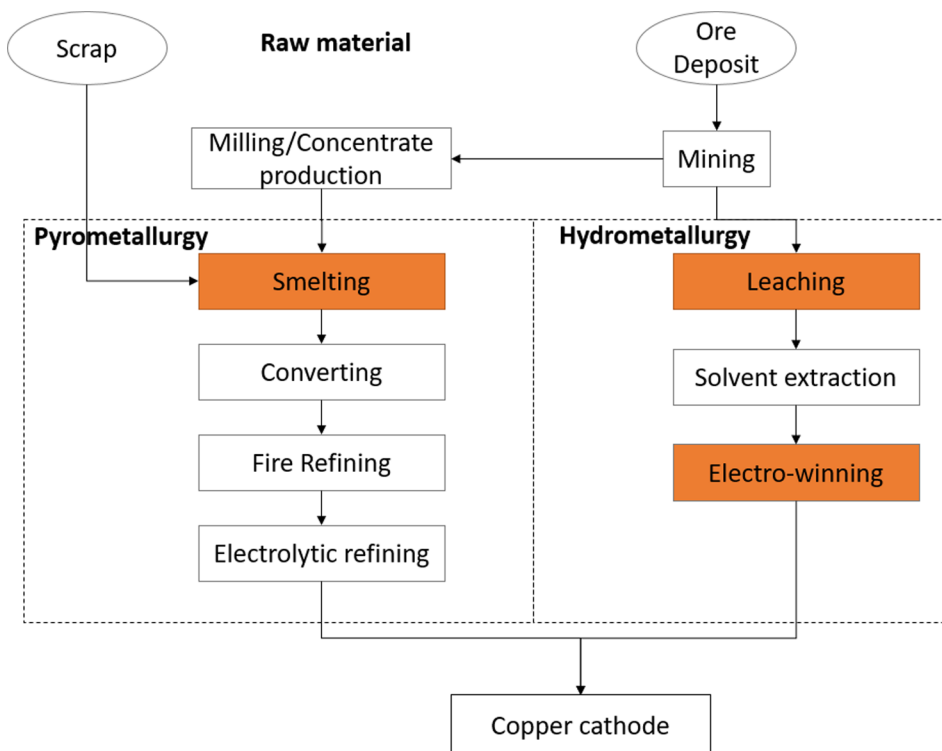


Fig. 3. Cooper mining production processes (European Copper Institute, 2018).

insufficient funding schemes, hindering the development of the solar thermal industry (Haas et al., 2018). Nonetheless, during the latest years, Chile has become a leader in Latin America in terms of the deployment of photovoltaic solar energy. The main reason for such developments is the large solar resource available in Chile, as well as favorable market conditions. The high levels of solar radiation are explained by the particular geographical and climate conditions, especially the northern and central Chile, which is where the main copper mining facilities are located. Northern Chile is endowed with an extremely dry climate characterized by the absence of precipitation and extreme temperatures with large-temperature oscillations between day and night, which allows reaching in this region yearly GHI levels between 2400 and 2800 kWh/m², while central Chile presents yearly GHI between 1800 and 2400 kWh/m², and a temperate climate, where the exception is the high terrains at the Andes mountains. The match between high radiation levels and the location of the copper facilities characterizes an exceptional opportunity for implementing solar energy technologies (Zurita et al., 2018), representing also a significant potential for solar energy projects (Fig. 5) in central and northern Chile (Escobar et al., 2015).

In copper mining, the production processes depend on the raw materials being processed: sulfides, or oxides. Sulfide processing is called pyrometallurgy, while oxide processing is called hydrometallurgy (Gallo et al., 2015), both processes are shown in Fig. 3, where in orange is shown the process that heat is required. In general, both processes used heat in different temperature ranges. In sulfide processing, there are two processes where heat is used: smelting copper at temperatures higher than 1000 °C, hence, the potential for using solar heat is rather low; and drying. On the other hand, oxides used heat for the EW process and for leaching, in both process the copper mining heat consumption is estimated in 939,389 MWh (Cochilco, 2018). Murray et al. (2017) have studied the integration of different sizes between of solar thermal field at different rates of extraction, where was analyzed NPV and IRR. In EW, heat is used to maintain the electrolyte between 45 and 55 °C, temperatures, a range that is easily reachable by solar thermal technologies. Indeed, two solar thermal

plants have been installed in the Atacama Desert (northern Chile) to supply hot water for the EW processes in copper mining facilities. One solar thermal plant is called *Pampa Elvira Solar* (34 MW_{th}), which is composed of flat-plate collectors (FPC), located at the facilities of *Gabriela Mistral* mine (Avaria, 2013). The second solar thermal plant is *El Tesoro* (10 MW_{th}), which is composed of a solar field of parabolic trough collectors (PTC), located at the *Centinela* mining district, also in the Atacama Desert (Avaria, 2014).

Several studies have reported the potential for implementing solar energy technologies into copper mining facilities in Chile. Chandia et al. analyzed the technical feasibility of solar technologies (thermal and photovoltaic) integration in the copper mining processes, concluding that only EW and electrorefining (ER) processes are suitable for solar thermal collectors integration (Chandia et al., 2016). Cuevas et al. studied the integration of FPC and parabolic trough collectors (PTC) large-scale solar plants in EW of three Chilean mines (*Cerro Colorado*, *El Abra*, and *Zaldívar*) getting positive perspectives for its implementation for reductions in conventional fuel consumption when solar systems and conventional heaters are integrated (Cuevas et al., 2015). Moreno-Leiva et al. studied the environmental benefit of reducing the global warming potential (GWP) of integrating solar energy in the Chilean copper industry. According to the study, the integration of solar electricity in pyrometallurgical and hydrometallurgical processes can generate a reduction in the carbon emissions of 63% and 76%, respectively. However, this study does not consider the effect of using solar heating in mining processes, and its potential impact for reducing the GWP (Moreno-Leiva et al., 2017). Back in 2013, the Appsol Project was carried out (Aiguasol, 2014), as an initiative funded by the Chilean Government whose main goal was developing an open-access web tool to easily evaluate the economic feasibility of integrating solar thermal systems in the industrial sector, based on the information given by the user about location, annual fuel consumption and available surface area for solar field installation. This project delivers a simple tool to evaluate the integration of thermal solar energy technologies in different industries, considering the industrial processes characteristics, as an approach to evaluate its potential, but it does not consider important

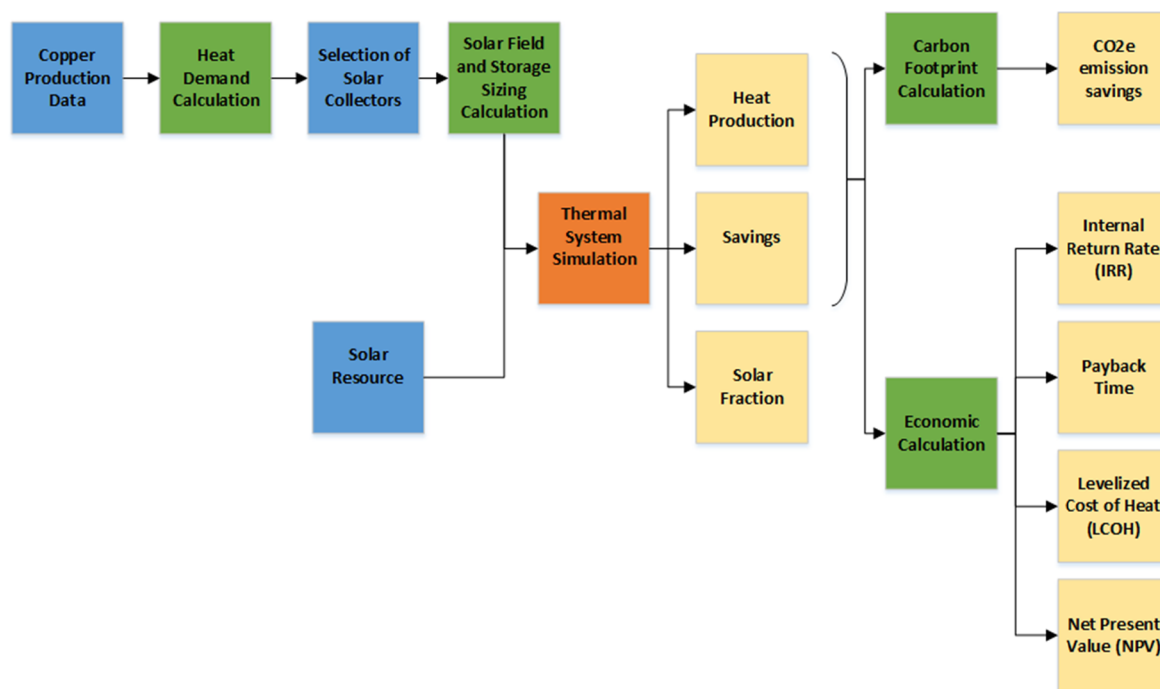


Fig. 4. Simulation diagram. The blue boxes denote the simulation inputs; the green boxes represent Matlab calculations; the orange boxes TRNSYS simulations; and the yellow boxes represent the simulations results. (For interpretation of the references to color in this figure legend, the reader is referred to the web version of this article.)

factors such as actual values to the economic analysis, the detailed solar resource available in the location, and a detailed simulation for each case.

Considering all of the previously discussed, there is a clear need for analyzing the benefits that can be obtained by large scale penetration of solar technologies for process heat supply into the copper mining industry in Chile. The present article presents an analysis of the integration of solar thermal technologies in EW process, taking as case studies the largest mining operations that utilize SX-EW refining processes. The results are shown in terms of technical, and economic potential, as well as CO₂ emissions reduction. Three technologies of solar collectors are evaluated: Flat plate collector (FPC), Evacuated tube collector (ETC) and Parabolic trough collector (PTC). The solar fraction for different solar field size, the Levelized Cost of Heat (LCOH), and the avoided CO₂ emissions are computed in a parametric analysis, depending on the GHI available at the specific location, while the economic analysis for payback time is also computed as a function of Oil prices. The study allows evaluating the potential for solar thermal utilization in a region especially attractive for solar projects, considering the high level of solar radiation available and the large heating demands, as described above. Hence, the present article aims to provide key information about the performance of solar thermal technologies coupled to EW processes, by conducting a detailed techno-economic assessment. These results would allow fostering the adoption of solar thermal technologies in the Chilean mining industry, by assessing its actual potential, and the methodology proposed can also be generalized in order to be applied to other regions in different countries where SX-EW copper production is being utilized by the mining industry.

2. Methodology

Modeling the introduction of solar heat to mining operations requires information about the process, solar resource, solar energy conversion technology, and costs. The process needs to be characterized in terms of its total heat demand, power, daily consumption profiles, and required temperatures. Fig. 4 shows the methodology diagram used in this article, where the thermal system simulation was done using TRNSYS 18.0 software (Klein et al., 2017), and the heat demand, solar and storage tank sizing, carbon footprint and economic calculations were carried out using MATLAB R2017a software (Mathworks, 2017).

The information about the process, the solar technology, and solar resource available allow simulating the system as is described in the next section, from which the heat production -both in total and in hourly profile, the solar fraction, and fuel savings are obtained. From those results, it can also be determined the CO₂ emissions reduction and the parameters that define the economic performance of the system, such as internal rate of return, payback time, net present value and LCOH.

Table 1

Annual copper cathodes production, annual solar irradiation, and location of mining with EW process in Chile.

Mine	Location	GHI (kWh/m ² /year)	DNI (kWh/m ² /year)	Production (FMT Cu)	Heat demand (MWh)
Antucoya	22.62 S, 69.83 W	2,595	3,409	66,200	51,226
Caserones	28.18 S, 69.53 W	2,330	3,094	30,000	23,214
Centinela	23.00 S, 69.09 W	2,622	3,457	55,800	43,178
Cerro Colorado	20.06 S, 69.26 W	2,561	3,227	74,400	57,571
Collahuasi	20.97 S, 68.63 W	2,565	3,556	22,246	17,214
El Abra	22.00 S, 68.73 W	2,630	3,589	99,900	77,303
Escondida	24.29 S, 69.03 W	2,658	3,686	237,974	184,144
Gabriela Mistral	23.45 S, 68.81 W	2,631	3,513	121,700	94,171
Lomas Bayas	23.43 S, 69.49 W	2,555	3,179	80,100	61,981
Los Bronces	33.14 S, 70.28 W	1,982	2,226	223,400	172,867
Quebrada Blanca	21.00 S, 68.79 W	2,605	3,559	34,700	26,851
Radomiro Tomic	22.19 S, 68.86 W	2,635	3,588	318,255	246,266
Spence	22.80 S, 69.27 W	2,577	3,316	167,400	129,534
Zaldívar	24.14 S, 69.04 W	2,624	3,677	103,400	80,011
			Average	116,820	90,395

2.1. Copper production data

The copper production data for every company in Chile is available as free access data provided to the Chilean government and published through Cochilco (Cochilco, 2016). The data was analyzed with the detailed production process of every mine in Chile in order to identify the production obtained from EW processes. That production data is summarized in Table 1.

2.2. Heat demand calculation

According to the information from Cochilco from the annual report of copper mining statistics (Cochilco, 2016), the average specific heat demand to produce a metric ton of fine copper through EW process is 773.8 kWh (FMT Cu), this value is calculated using the reported values from years between 2001 and 2015. Table 1 shows the location, solar radiation availability and annual copper cathode production by mine facility that considers EW process for copper production in Chile. The copper mining industry commonly works 24/7, therefore the demand is assumed as constant throughout all of the year. Fig. 5 shows the solar resource over the Chilean territory, in addition to the specific locations of the copper mining facilities listed in Table 1.

2.3. Selection of solar collectors

Most industrial processes that require heat operate at temperatures between 40 and 250 °C (Kalogirou, 2004). In the case of the EW process, the electrolytic water-acid-copper solution needs to be kept at a temperature between 45 and 60 °C (Schlesinger et al., 2011). As the solar collector selection depends mainly on the operational temperature, cost, O&M requirements, and other factors such as land usage, this study considers the three main technologies commercially available. The main characteristics of the solar collectors considered for the present analysis are presented in Table 2, showing the typical temperature operation range for FPC, ETC, and PTC technologies, and their main parameters for the simulations. FPC and ETC are generally recommended to deliver heat up to 120–150 °C. PTC can reach higher temperatures, however, the need for a tracking system by PTC increases significantly its capital cost. The implementation of the different solar technologies in each of the mining facilities is analyzed herein, in order to evaluate its performance in terms of the financial yield and thermal performance.

2.4. Solar resource

The solar resource and weather conditions databases for conducting the simulations were taken from the *Solar Energy Explorer* web tool

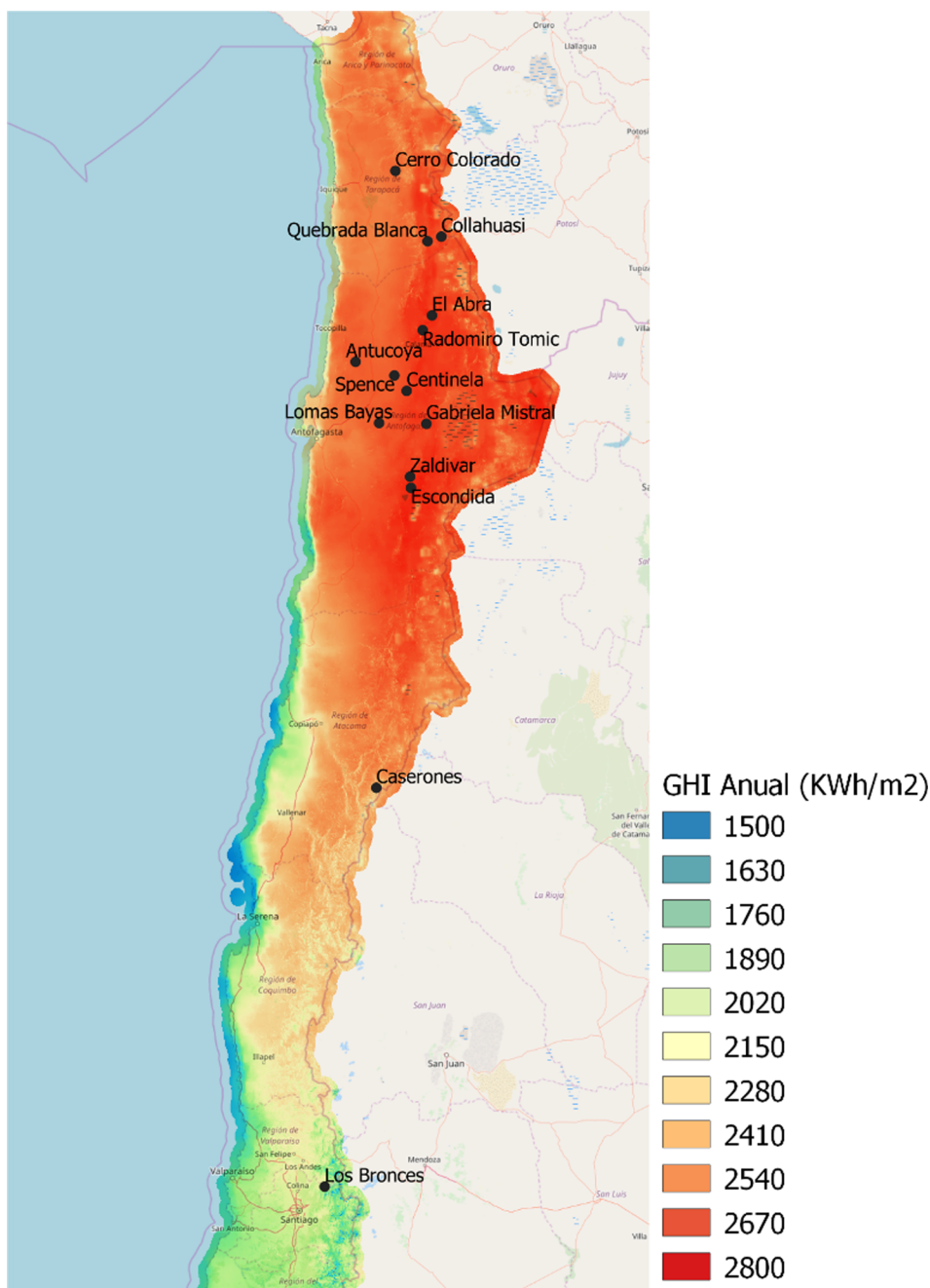


Fig. 5. Solar resource map with the copper mines evaluated.

(Department of Geophysics - University of Chile and Ministry of Energy, 2012). That tool provides hourly information from a satellite estimation model that has processed long term data with the time series starting in 2004, including solar radiation (GHI, DNI, and diffuse horizontal irradiation (DHI)) and site meteorological conditions (temperature and wind velocity). Considering such information, a typical meteorological

year (TMY) dataset is configured, which is integrated into the simulation deck in TRNSYS.

The data provided by the *Solar Energy Explorer* web tool is based on satellite measurements, combining it with models that process the solar irradiation, which is modified through the atmosphere, building high temporal and spatial fields of incident solar irradiation. The temporal

Table 2
Operational temperature ranges of different solar collectors (Solar Keymark, 2016; TÜV Rheinland, 2016; Weiss and Rommel, 2008).

Collector	Type	Temperature range (°C)	$F_R(\tau\alpha)_n$	$F_R(U_L)$ (W/m ² K)	$F_R(U_L/T)$ (W/m ² K ²)
Flat plate	HT-HEATboost 35/10	40–120	0.779	2.41	0.015
Evacuated tube	Vitosol 200-TM CP1A 18 Tubes	80–180	0.484	0.749	0.009
Parabolic trough	PT-1	100–450	0.66	0.48	0.003

series are in an hourly format, and this information was validated using ground measured data from 131 solarimetric stations that measure GHI throughout the Chilean territory. From these solarimetric stations, 67 correspond to the first category standard with better data quality and good ground coverage in Chilean territory, to allow the validation of the model developed from satellite data.

To validate GHI the daily total irradiation was calculated in all data periods, for all the solarimetric stations, this value is compared with the results simulated by the model for the same time series. This analysis separates the Chilean territory in 3 zones: North from latitude 17° S to 30° S, Central from latitude 30° S to 40° S, and South from latitude 40° S to 56° S. For each zone was calculated its mean bias and root mean square error (RMSE) between the data measured and the model, results are shown below (Department of Geophysics - University of Chile, 2017).

Most of the locations considered for this work are located in the Northern Region, and one is located in the Central Region of the aforementioned classification for the validation process. In Table 3 is shown the Quantity of solar resource stations, Mean bias and RMSE. In the Northern Region, the model for GHI used by the Solar Energy Explorer presents a bias lower than 5% for clear sky irradiation, but for cloudy sky irradiation, the model tends to overestimate the irradiation. This effect is due to an underestimation of the cloudiness in the region. These errors do not affect significantly the statistical results of the model due to the low frequency of clouds in the zone, resulting in a bias nearby to zero at this zone. In the Chilean Central Region, the model represents well both clear and cloudy skies. For clear-sky conditions, at all stations, the bias is lower than 10%, and just 15% of the stations have bias higher than 10% at cloudy hours. The mean bias of the complete hourly series is lower than 10% in every station. Fig. 6 shows the mean measured GHI for each station utilized in the validation process of the Solar Energy Explorer against the modeled GHI at the same location. The dotted lines represent the limit difference of 10% (Department of Geophysics - University of Chile, 2017).

Finally, to validate the DNI there is only one station located in the Northern Region (Crucero, Lat 22.20° S and Lon 69.29° W) that measures directly DNI. In this case, the total daily irradiation is calculated to be compared with the results of the model for the same period at hourly series, resulting in a mean bias of 5.5% and RMSE of 15% for hourly data. There are 11 stations that measure global and diffuse irradiation using horizontal single-axis tracking (HSAT). Using these stations the HSAT direct irradiation was calculated and performed the validation for the DNI in the model. The results show that for the HSAT direct irradiation at these 11 stations the mean bias is 4% and the RMSE 11% for hourly series, similar to the results obtained in the analysis of Crucero measured DNI (Department of Geophysics - University of Chile, 2017). The locations where there are higher differences correspond to the locations with high cloudy frequency, at these locations the model presents higher errors, but that errors are not observed at the locations of the plants analyzed in this work.

2.5. Solar field and storage tank sizing

Ten different sizes of the solar system were evaluated for each mining facility, considering for each line of collectors 10, 10 and 4 collectors in series for FPC, ETC and PTC respectively. The volume of the storage tank was also assessed, changing according to the same ratio between storage tank volume (in liters) and solar field area (in m²) that the observed in the reference plant: “Pampa Elvira Solar” (110 L/m²). The objective is to analyze the impact of the performance parameters when evaluating different solar field area and storage tank volumes. The ten sizes chosen for each mine were evaluated as fractions of the minimum size to supply 100% of energy demand for the EW process. It was considered sizes from 10 to 100% of that value, increasing 10% for each case evaluated until reaching 100%. The calculation of the solar field was performed considering the following equation depending on

the heat demand.

$$A_{total} = \frac{j * dda}{RAD * \eta_{coll}} \quad (1)$$

where j is the solar fraction expected, dda is the heat demand, η_{coll} is the efficiency expected of the solar thermal system (assumed in 52%) and RAD is the annual solar irradiation in the location (for FPC and ETC is used GHI and for PTC is used DNI estimations).

2.6. Thermal system simulation

The configuration of the solar arrangement analyzed herein was developed considering a common installation for the mining industry, such as the scheme implemented for the EW process in “Pampa Elvira Solar” and “Minera El Tesoro” (Fig. 9) (Abengoa Solar, 2017; E-Llaima, 2017). Such scheme was configured in a TRNSYS deck and simulated on an hourly basis, allowing to assess its annual performance. The scheme is depicted in Fig. 7, where the solar system is composed by a solar collector field and a single-speed pump, using a mixture of water and 33% w/w propylene glycol as a working fluid for FPC and ETC collectors with a specific heat capacity of 3.824 kJ/kgK, or water as a working fluid for the PTC with a specific heat capacity of 4.18 kJ/kgK. The solar circuit transfers its energy gain for heating up water in a stratified storage tank through a heat exchanger (HX(1)). Then, the water from the top of the storage tank is pumped to the process heat exchanger (HX(2)). A conventional water heater integrated into a parallel-serial configuration that complements the energy demanded, in order to ensure the temperature required by the processes. The water heater is evaluated using a simplified model, which is controlled by the required process temperature and does not consider variations on the efficiency due to partial load operation. Finally, the warm water delivers energy to the process water, through the process of heat exchanger (HX(3)). All the collector technologies analyzed herein are modeled considering the same integration scheme for the location of each mining facility analyzed.

The system is mainly controlled through the activation of the circulating pumps. The solar field circuit is controlled by a differential temperature controller, which activates the circulation pump when the collector's output temperature is higher than the temperature at the bottom of the storage tank. The temperatures at the top of the tank and collector's outlet are monitored during the operation, then this information is considered to switch off the circulation pump when the tank temperature exceeds 100 °C. In addition to that, the controller was configured considering two dead-band temperatures (2 and 10 °C, for lower and upper-temperature dead-band, respectively). The results of the monthly solar heat production, fuel consumption, and energy demands are used for performing an economic assessment evaluation. Table 4 summarizes the main parameters considered by the simulation model in TRNSYS.

Different components (Types) were used for the TRNSYS simulation, where each Type describes the behavior of a subsystem using mathematical or thermodynamic models. The components used for the TRNSYS simulation, and the main parameters are summarized in Table 5.

Table 3

Mean bias and RMSE at each zone per solar resource measurement station (Department of Geophysics - University of Chile, 2017).

Region	Quantity of solar resource stations	Mean bias (%)	RMSE (%)
North	24	−1.3	5.7
Central	26	−0.4	9.6
South	17	0.9	16.7
Total	67	−0.38	10.0

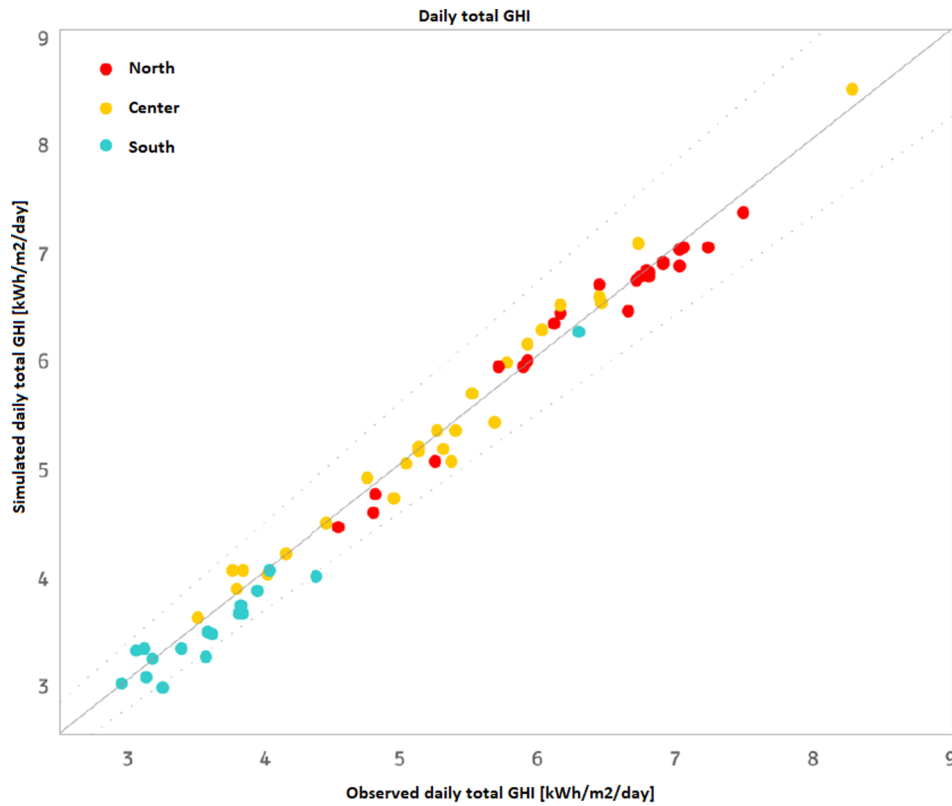


Fig. 6. Scatter plot between Observed and Simulated daily total GHI (Department of Geophysics - University of Chile, 2017).

2.7. Heat production

The heat production of the solar-EW scheme was determined by performing the simulations in TRNSYS for every technology and location analyzed, considering the parameters mentioned in the previous

sections. These results are analyzed in terms of an hourly, monthly and annual basis, allowing to perform the thermodynamic and economic analysis for each of the scenarios analyzed.

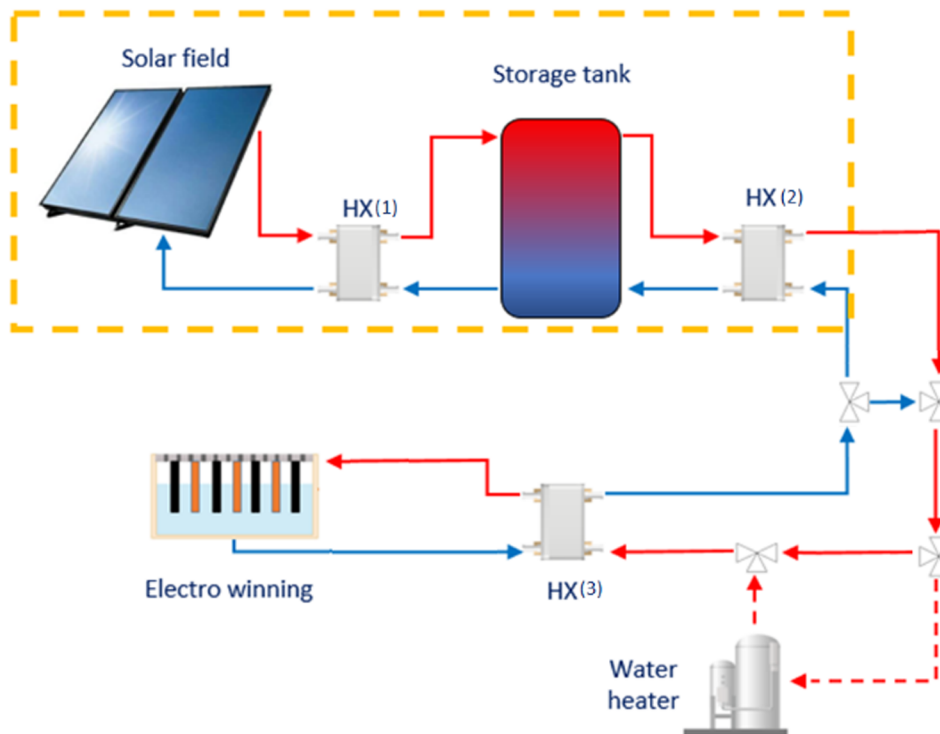


Fig. 7. Integration scheme for EW process.

Table 4
Model input parameters for TRNSYS simulation.

Solar field and storage	Mining industry
Solar collector technology	Hourly production profile
Solar collector efficiency parameters	Input and return temperatures of the processes
Solar field size	Mass flow rate
Storage capacity	
Solar radiation for each location	

2.8. Fuel energy savings

Fuel savings refer to fuel consumption savings. This value is estimated as the percentage between the fuel consumed originally and the fuel consumed after the integration of the solar system. Thus, the fuel savings are represented as follows,

$$S = 1 - \frac{\left(S_{fuel} - \frac{E_{Solar}}{\eta_{heater} \cdot C_{fuel}} \right)}{S_{fuel}} \tag{2}$$

where S is the annual fuel saving in terms of the fuel displaced by the solar thermal system, which is represented as a percentage of the fuel originally consumed by the plant, S_{fuel} is the fuel consumption by the fossil system without the contribution of the solar plant, E_{Solar} is the solar thermal energy delivered that is effectively used by the process, η_{heater} is the heater efficiency, which is assumed to be approximately 78% (IEA-ETSAP, 2010), for a conventional oil water heater, and C_{fuel} is the heat from the fuel combustion, corresponding to the lower heating value, which is assumed as 10.63 MWh/m³ (Agencia Chilena de Eficiencia Energética, 2011).

2.9. Solar fraction

The solar fraction represents the rate of energy that is provided by the solar field to the plant. It is estimated as a ratio between the energy provided by the solar field E_{Solar} and the total energy required for the plant at nominal conditions E_{Total} , which corresponds to the sum of the energy provided by the solar field and the energy provided by the fossil system.

$$S_{fraction} = \frac{E_{Solar}}{E_{Total}} \tag{3}$$

2.10. CO₂ emissions

As a measure of the performance of the solar systems, it is evaluated the CO₂ emissions reduction, when compared to an EW process-driven fully by fossil fuel heaters. In that context, the total CO₂ emissions (expressed in tons of CO₂e), associated with the use of fossil fuel is determined by the following equation:

Table 5
Model input parameters for TRNSYS simulation (Solar Keymark, 2016; TÜV Rheinland, 2016; Weiss and Rommel, 2008).

Component	TRNSYS Type	Parameter	Value	Unit
Flat plate collector	1c	$F_R(\tau\alpha)_n$	0.779	–
		$F_R(U_L)$	2.41	(W/m ² K)
		$F_R(U_L/T)$	0.015	(W/m ² K ²)
Evacuated tube collector	71	$F_R(\tau\alpha)_n$	0.484	–
		$F_R(U_L)$	0.749	(W/m ² K)
		$F_R(U_L/T)$	0.009	(W/m ² K ²)
Parabolic trough collector	536	$F_R(\tau\alpha)_n$	0.66	–
		$F_R(U_L)$	0.48	(W/m ² K)
		$F_R(U_L/T)$	0.003	(W/m ² K ²)
Heat exchangers	91	HX Effectiveness	0.7	–
Storage tank	158	Loss Coefficient	0.923	(W/m ² K)

Table 6
Economic assumptions.

Parameter	
Diesel (tax free) (USD/MWh _{th})	53.88
Electric power (USD/MWh)	99
Discount rate	10%
Evaluation period (years)	20
Inflation	2.24%
Range of FPC cost min ~ max (USD/m ²)	330–687
Range of ETC cost min ~ max (USD/m ²)	460–817
Range of PTC cost min ~ max (USD/m ²)	379–1,263
Storage tank cost (USD/m ³)	2,000
O&M cost	2% of investment

$$G_f = E_f E_{Ff} \tag{4}$$

where, E_f is energy produced by fuel consumption in TJ, E_{Ff} is fuel emission factor in tons C/TJ. For the current analysis Diesel oil is considered as the back up fuel, which has a CO₂ emission factor of 0.2496 Tons of CO_{2e}/MWh (U.S. Energy Information Administration, 2016).

2.11. Economic figures

To determine the economic viability for each configuration/technology, the results were compared based on the following economic indicators: net present value (NPV), intern rate of return (IRR), payback time, and the Levelized Cost of Heat (LCOH).

The NPV is defined by the following equation:

$$NPV = I - \sum_{j=1}^N \frac{F_j}{(1 + d)^j} \tag{5}$$

where I corresponds to the investment cost in the first period, F_j is the net annual cash inflow-outflow considering inflation, j represents the period and d represents the discount rate.

The IRR corresponds to the value of the discount rate that for the period of evaluation for the project results in NPV equal to zero. Hence the IRR is calculated from the next equation:

$$0 = I - \sum_{j=1}^N \frac{F_j}{(1 + IRR)^j} \tag{6}$$

The payback time is calculated counting the last period with a net annual cash inflow-outflow negative denominated A , and adding to it the absolute value of cumulative net cash flow at the end of this period denominated B , divided by the total cash inflow during the following period denominated C , as is shown in the following equation:

$$Payback = A + \left| \frac{B}{C} \right| \tag{7}$$

The LCOH was evaluated according to the definition established by Louvet et al. (2017):

Table 7
Model validation comparison.

	El Tesoro			Pampa elvira solar		
	Public data	TRNSYS model	Difference	Public data	TRNSYS model	Difference
Collector	PT-1			HT Heat Boost 35–10		
Solar field surface (m ²)	16,742	16,742	–	39,300	39,300	–
Storage size (m ³)	300	300	–	4,300	4,300	–
Annual heat production (MWh _{th})	24,845	23,225	7%	54,000	52,568	3%
Solar Fraction	55.60%	53.79%	3%	55.83%	54.35%	3%
Fuel savings	55%	54%	2%	80%	79%	1%
CO ₂ e emission savings (ton)	7,951	7,432	7%	15,000	16,823	12%
Yearly sum of DNI (El Tesoro) and GHI (Pampa Elvira) (MWh)	~53,058	52,096	2%	~97,500	101,832	4%



Fig. 8. Solar thermal plants for the mining industry in Chile. Fig. 6a and b show Pampa Elvira Solar. Fig. 6c and d show El Tesoro (Ellaima, 2015; Futuro Renewable, 2014; Interempresas, 2013).

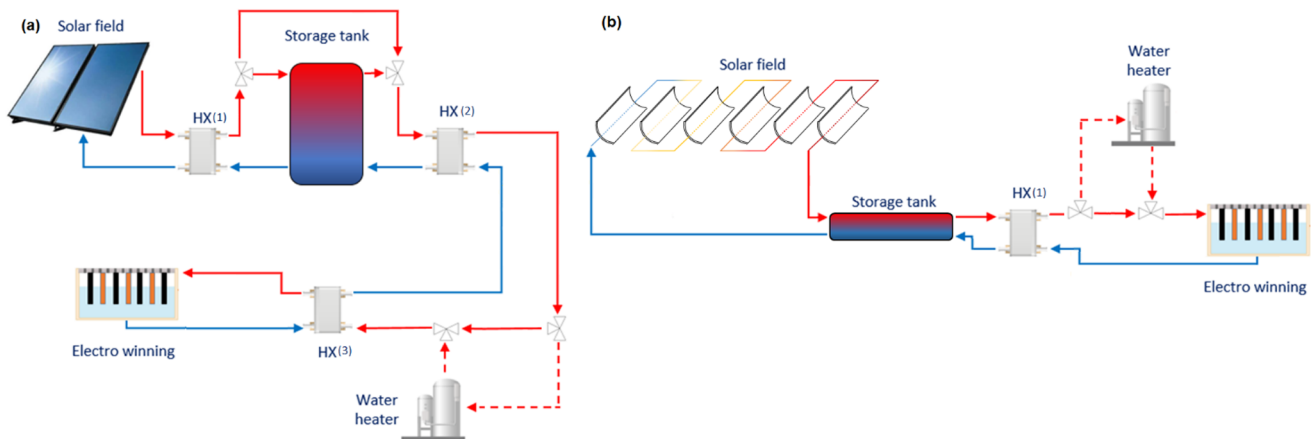


Fig. 9. Integration diagram for the solar thermal plant in: (a) Pampa Elvira, (b) El Tesoro.

$$LCOH = \frac{\sum_{j=0}^N (I + C_{O\&M}) \frac{(1+i)^j}{(1+d)^j}}{\sum_{j=0}^N Q_j \frac{(1+i)^j}{(1+d)^j}} \quad (8)$$

where I is the investment cost, $C_{O\&M}$ is the operational and maintenance cost, and Q_j is the heat generated during the j period, i is the inflation rate and d is the discount rate.

2.12. Assumptions

The simulations were carried out considering FPC, ETC, and PTC, where the slope of the fixed collectors (FPC and ETC) is assumed as equivalent to the location’s latitude. Table 6 summarizes the economic parameters taken into consideration for the economic assessment.

In order to represent a realistic situation for the heating process in a

Table 8
Copper mine, solar field, and storage tank ranges.

Location	Collector	Solar field area range (m ²)	Thermal storage tank range (m ³)
Antucoya	FPC	3,826–38,240	418–4,183
	ETC	3,825–38,240	418–4,183
	PTC	2,869–26,234	286–2,866
Caserones	FPC	1,940–19,310	211–2,111
	ETC	1,935–19,305	211–2,111
	PTC	1,639–15,576	166–1,663
Centinela	FPC	3,202–31,903	348–3,489
	ETC	3,190–31,900	348–3,489
	PTC	2,459–21,725	235–2,354
Cerro Colorado	FPC	4,355–43,546	476–4,764
	ETC	4,355–43,545	476–4,764
	PTC	3,279–30,744	334–3,345
Collahuasi	FPC	1,302–13,013	142–1,422
	ETC	1,305–13,005	142–1,422
	PTC	1,229–9,428	99–999
El Abra	FPC	5,699–56,953	623–6,230
	ETC	5,695–56,950	623–6,230
	PTC	4,099–39,352	426–4,264
Escondida	FPC	13,421–134,207	1,468–14,684
	ETC	13,425–134,205	1,468–14,684
	PTC	9,018–89,363	975–9,755
Gabriela Mistral	FPC	6,934–69,342	758–7,586
	ETC	6,935–69,335	758–7,586
	PTC	4,919–46,730	509–5,093
Lomas Bayas	FPC	6,934–69,342	4,708–47,006
	ETC	6,935–69,335	4,705–47,005
	PTC	4,919–46,730	3,689–33,613
Los Bronces	FPC	16,894–168,932	1,848–18,482
	ETC	16,895–168,825	1,848–18,482
	PTC	13,527–134,043	1,464–14,648
Quebrada Blanca	FPC	2,008–19,975	218–2,184
	ETC	2,000–19,970	218–2,184
	PTC	1,369–13,937	148–1,489
Radomiro Tomic	FPC	18,115–181,037	1,980–19,806
	ETC	18,105–181,030	1,980–19,806
	PTC	12,707–123,385	1,347–13,473
Spence	FPC	9,743–97,378	1,065–10,654
	ETC	9,740–97,375	1,065–10,654
	PTC	6,968–67,226	733–7,335
Zaldivar	FPC	5,916–59,070	646–6,462
	ETC	5,910–59,065	646–6,462
	PTC	4,099–40,992	446–4,464

copper mining facility, a diesel price of 53.88 USD/MWh_{th} (tax-free) was considered, since the high consumption that copper processing facilities present allows them to directly import fuel. This value was defined according to the annual average price reported in ENAP (2018), and considering the Diesel oil properties reported in AChEE (2018). The inflation rate considered is based on the report from Inflation (2017). Regarding the collector costs, the values are based in 2016 Dollars, adjusted considering inflation. FPC ranges from the specific cost of large-scale systems in Denmark (> 50,000 m²) (Weiss and Spörk-Dür, 2018) to the specific cost of Pampa Elvira Solar, where the investment cost was determined from publicly available data (MiningPress, 2013). ETC costs are estimated as 130 USD/m² more expensive than the FPC, as observed in several market prices studies and suggested by Dietram et al. (2013). The PTC costs are based on the range reported by International Renewable Energy Agency (2015). All the collector prices consider BoS costs; and the costs of the storage tank were taken from the reported in Sisó and Gavalda (2009).

2.13. Model validation

The TRNSYS deck developed was validated using public data from two solar thermal plants installed in Chile, Pampa Elvira Solar (Olivares S., 2016) and Planta Solar El Tesoro (Román et al., 2014). Table 7 shows a comparison between the data and the results delivered by the TRNSYS

model. The simulations were carried out using the efficiency parameters for the solar collector listed in Table 2; and the meteorological conditions from the Solar Energy Explorer. It can be inferred from the results that both models are representative of the annual heat production with acceptable accuracy, compared to the public data. Showing differences lower than 10% for most of the performance parameters, which is considered as acceptable considering the low information available. Fig. 8 shows actual pictures of the “El Tesoro” and “Pampa Elvira Solar” solar projects, and Fig. 9 shows a diagram of the integration scheme for each installation. Those schemes represent the simulations evaluated during the validation procedure and later considered as a reference scheme for the present study.

3. Results

Four analyses were carried out, aiming to assess the actual potential for implementing solar thermal technologies in copper mining facilities in Chile. In a first place, it was estimated the LCOH (1) of a solar thermal plant coupled to different copper mining operations, that currently have operating an EW process as part of the production plant. A parametric analysis was carried out for assessing the impact of solar radiation and the solar field size on the LCOH (2), and CO_{2e} emissions (3). Finally, it was also carried out a sensitivity analysis (4) of collector and oil prices over the LCOH, aiming to evaluate its competitiveness in different scenarios. For these cases, a thermodynamic analysis was performed using TRNSYS simulations, allowing to evaluate the heat delivered to the process, when the solar system is integrated.

3.1. Integration in mines with EW plants in Chile

An energetic analysis of the mining operations listed in Table 1 was carried out using TRNSYS software, in terms of the thermal energy supplied from the solar systems. That software allows running hourly simulations and estimating the total heat production of the solar plant, considering the three different technologies studied herein, and 10 different solar field sizes, as listed in Table 8. The heat delivered represents a fraction of the total heat demand from the EW plant in each of the mining operation analyzed. Moreover, considering the heat production estimated in every case, and the economic parameters presented in Table 6, an economic evaluation based on the LCOH was carried out. In this analysis two approaches for determining the LCOH were considered, corresponding to the extreme values of the cost ranges given in Table 6, for the three collector technologies. The simulations were performed considering the simulation schemes described in the previous section.

Fig. 10 shows the results of the economic analysis in terms of the LCOH for each location. The circle sizes represent the solar field area in each case, and the circle center point represents the LCOH. There are ten different solar field area for each case. It is worth to mention that for determining the LCOH, the CAPEX is assumed equivalent to the cost of the solar field and the costs of the storage tank installed. On the other hand, the OPEX is considered equivalent to 2% of the CAPEX. These results show two values of LCOH corresponding to the minimum and maximum costs for the collectors, as specified in Table 6. It is observed that in the case of PTC the LCOH value is almost not affected by the size of the solar field, in difference with the other technologies.

In Fig. 10, the LCOH of the heat delivered by the solar systems is compared to an approximated value of the LCOH when a diesel water heater is considered, which is the most common technology used nowadays in the EW process. That approximated LCOH value considers the cost of diesel presented in Table 6 (53.88 USD/MWh) and such value is evaluated assuming a constant efficiency of 78% for the water heater. Thus, the approximated value for the diesel driven LCOH turns to be 69.07 USD/MWh. Moreover, considering the maximum and minimum value for diesel in Chile during 2018, corresponding to 61.52 USD/MWh and 46.6 USD/MWh respectively, the LCOH ranges between

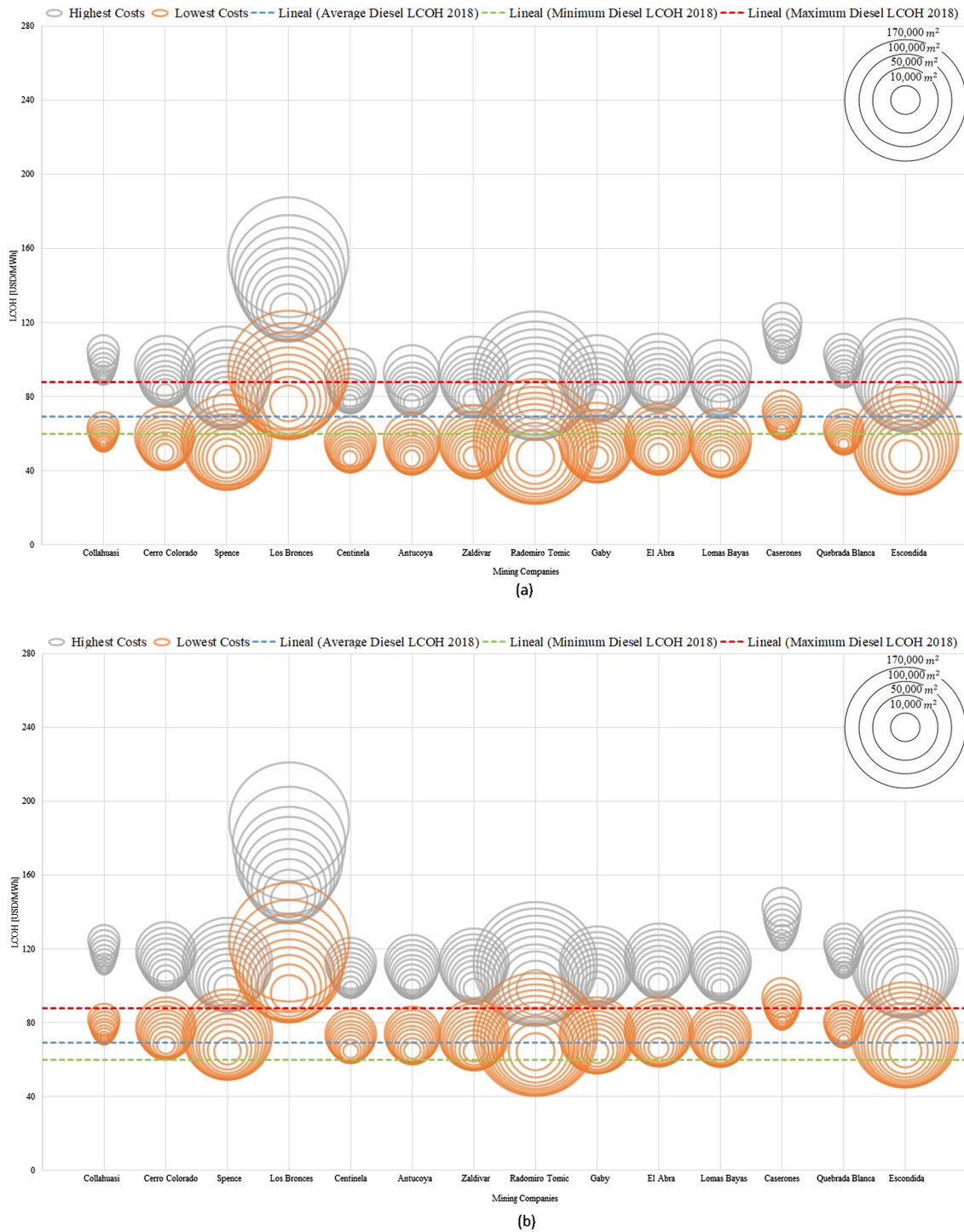


Fig. 10. LCOH for solar technologies compared to diesel costs, evaluating ten different sized of the solar field for each technology. (a) FPC; (b) ETC; (c) PTC.

87.88 USD/MWh and 59.74 USD/MWh. Those values are presented in Fig. 10 as dotted lines, showing the relevance in diesel prices for the economic feasibility of the solar technologies in this case, and defining a range where solar technologies are economically feasible.

The highest LCOH per mining facility and solar technology observed in Fig. 10, corresponds unsurprisingly to the cases where the maximum costs of all plant components were selected. From Fig. 10, it was obtained the lowest and highest values of LCOH per solar technology and mine. Table 9 presents a summary of the solar fraction, payback time and CO₂ emission savings considering the cases with the lowest LCOH values per solar technology and location. To calculate the LCOH in this

analysis it is assumed for the cost of the solar collectors an average value from the values presented in Table 6. The lowest LCOH values reached by each technology, in most cases, were obtained when considering the lowest solar field size evaluated, being the FPC the technology that achieves the lowest LCOH values, in contrast with the PTC technology. In the cases of FPC and ETC technologies, the solar field area corresponding to the lowest LCOH was the smallest solar field area, but in the case of PTC technology, this is not a trend. In the case of PTC technology, the LCOH is almost independent of the solar field area, mainly due to the high increase on the heat production by the solar field when its size increases, for this reason, the values presented in Table 9

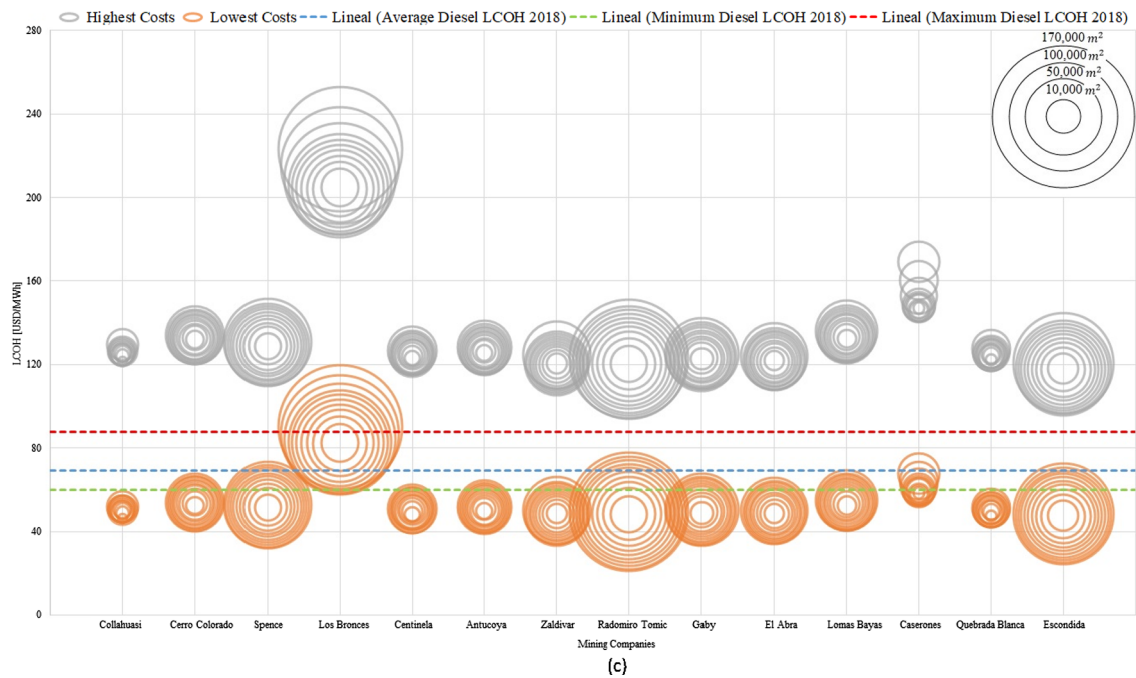


Fig. 10. (continued)

Table 9

Lowest level of LCOH obtained for each technology and mine.

Location	Collector	Solar field area (m ²)	Solar fraction	Payback (years)	LCOH (\$/MWh)	CO2e savings (ton)
Antucoya	FPC	3,826	10%	8	61.8	1,712.10
	ETC	3,825	9%	11	82	1,521.70
	PTC	2,869	8%	12	87.6	1,270.50
Caserones	FPC	1,940	9%	11	82.5	649.5
	ETC	1,935	8%	14	101.5	621.4
	PTC	3,279	17%	14	102.2	1,248.30
Centinela	FPC	3,202	10%	8	62	1,426.40
	ETC	3,190	9%	11	81.6	1,274.20
	PTC	2,459	8%	11	85.7	1,104.80
Cerro Colorado	FPC	4,355	10%	9	66	1,825.80
	ETC	4,355	9%	11	85.7	1,657.00
	PTC	3,279	8%	12	92.3	1,384.30
Collahuasi	FPC	1,302	9%	10	72.5	496.7
	ETC	1,305	9%	12	90.1	471.8
	PTC	1,229	10%	11	83.9	547.9
El Abra	FPC	5,699	10%	9	65.4	2,409.10
	ETC	5,695	9%	11	83.6	2,219.90
	PTC	8,198	15%	11	84.9	3,775.30
Escondida	FPC	13,421	10%	8	63.3	5,865.40
	ETC	13,425	9%	11	81.4	5,379.50
	PTC	27,055	22%	11	82.5	12,935.50
Gabriela Mistral	FPC	6,934	10%	8	62.3	3,079.60
	ETC	6,935	9%	11	81.2	2,782.80
	PTC	4,919	7%	11	85.9	2,238.50
Lomas Bayas	FPC	4,708	11%	8	61.4	2,119.00
	ETC	4,705	9%	11	81.7	1,876.70
	PTC	3,689	8%	12	92.4	1,547.90
Los Bronces	FPC	16,894	8%	14	101.2	4,616.90
	ETC	16,895	8%	17	121.5	4,532.50
	PTC	53,699	27%	> 20	143.2	14,808.20
Quebrada Blanca	FPC	2,008	9%	9	72	770.2
	ETC	2,000	8%	12	89.3	729.7
	PTC	1,639	9%	11	84.9	735.7
Radomiro Tomic	FPC	18,115	10%	8	62.7	7,995.80
	ETC	18,105	9%	11	81.3	7,259.20
	PTC	12,707	8%	11	84.3	5,920.70
Spence	FPC	9,743	11%	8	61.3	4,396.90
	ETC	9,740	9%	11	81.5	3,897.40
	PTC	20,496	22%	12	90.2	8,944.80
Zaldivar	FPC	5,916	10%	8	63.2	2,589.20
	ETC	5,910	9%	11	81.5	2,363.60
	PTC	16,396	30%	11	84	7,705.40

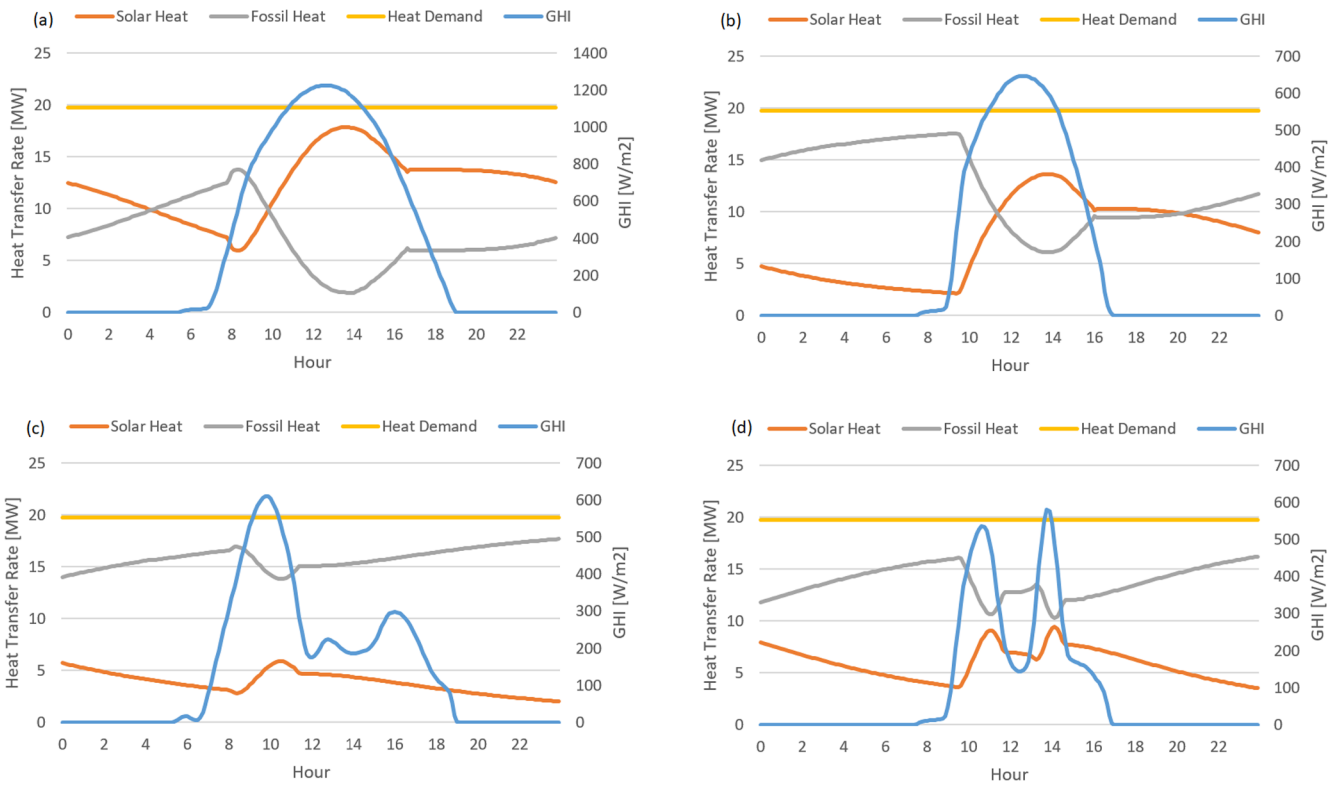


Fig. 11. Daily performance of an FPC plant at “Los Bronces”, considering four different days. (a) Clear Sky Day in summer (b) Clear Sky Day in winter (c) Cloudy Day in summer (d) Cloudy Day in winter.

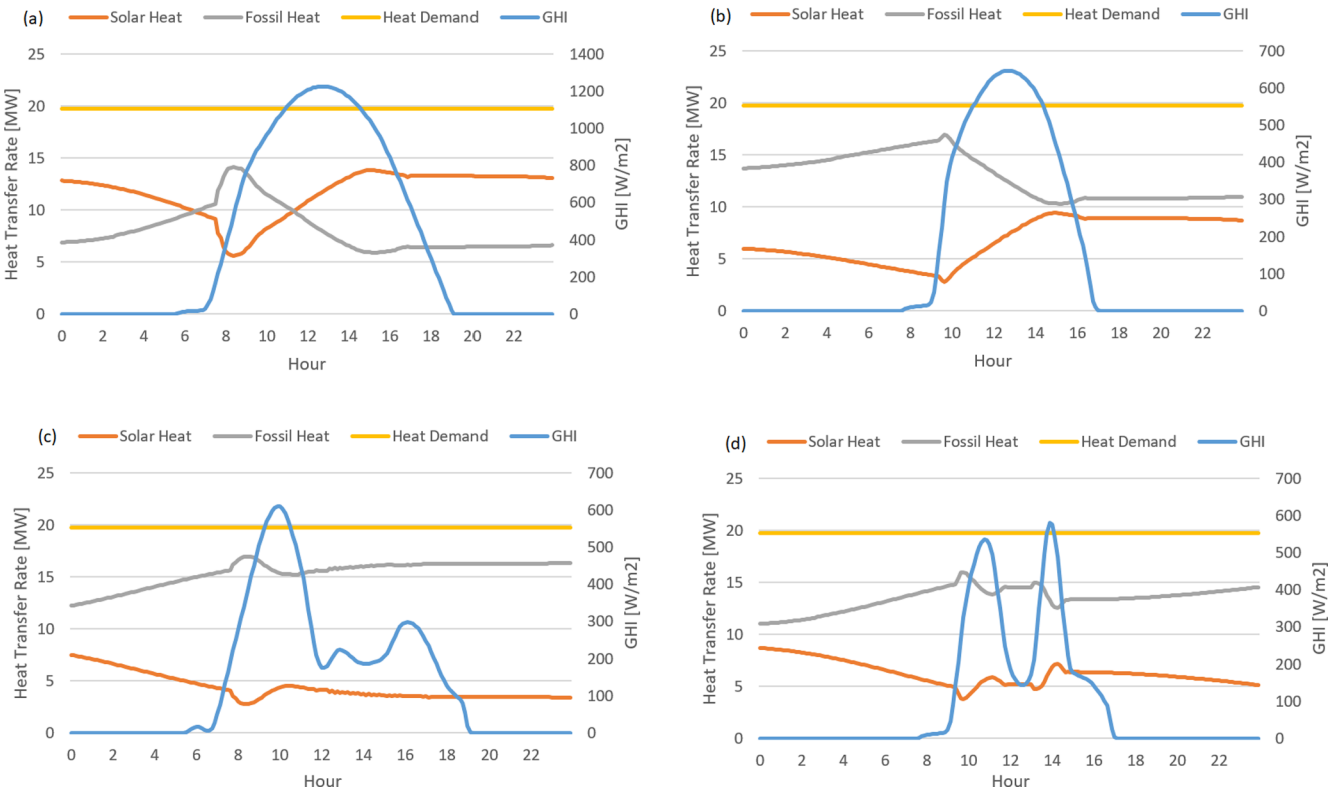


Fig. 12. Daily performance of an ETC plant at “Los Bronces”, considering four different days. (a) Clear Sky Day in summer (b) Clear Sky Day in winter (c) Cloudy Day in summer (d) Cloudy Day in winter.

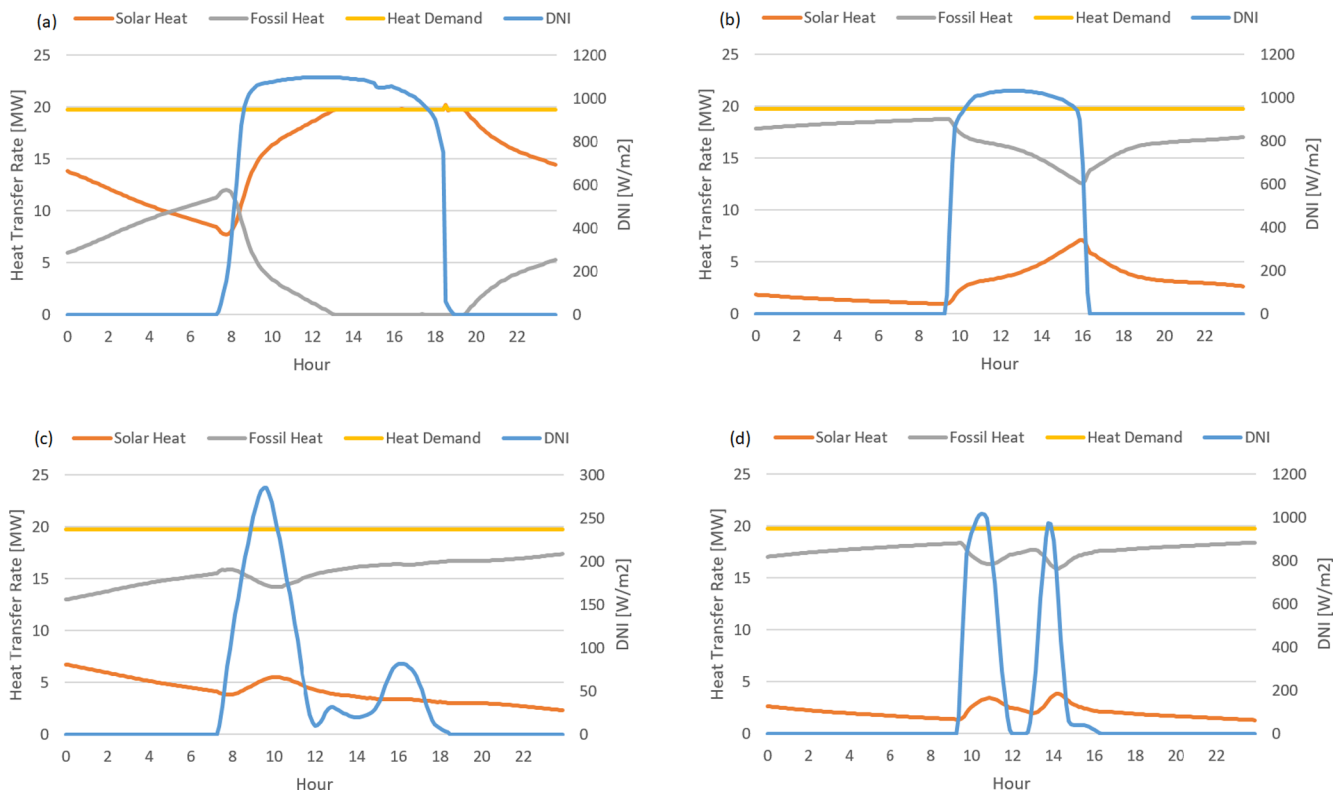


Fig. 13. Daily performance of a PTC plant at “Los Bronces”, considering four different days. (a) Clear Sky Day in summer (b) Clear Sky Day in winter (c) Cloudy Day in summer (d) Cloudy Day in winter.

Table 10
Daily solar fraction for each technology for cloudy and clear sky days.

Technology	FPC	ETC	PTC
Solar fraction clear sky day in summer (9th January)	62.82%	58.89%	77.49%
Solar fraction cloudy day in summer (5th January)	19.49%	21.95%	21.04%
Solar fraction clear sky day in winter (8th July)	37.04%	34.29%	14.61%
Solar fraction cloudy day in winter (9th July)	29.98%	31.74%	10.53%

are not coincident with the smallest solar field area for the PTC technology. For FPC and ETC technologies, in almost every case the payback time is nearby to 10 years, except for “Los Bronces”, because this location receives lower annual GHI and DNI.

A deeper analysis of the plant’s performance under different meteorological conditions was applied to “Los Bronces”, the location that presents the lowest solar resource. This location was selected due to the

high variation of the solar resource and a large number of cloudy days observed during the year. In this context, four days are evaluated for each technology where those days represent different conditions in terms of solar irradiation. The first day evaluated corresponds to January 9th, which corresponds to a clear-sky day during summer where the solar radiation is stable during the day. The second day corresponds to January 5th, which corresponds to a cloudy day in summer, showing high variability on the solar resource during the day. The third day evaluated corresponds to July 8th, which corresponds to a clear sky day during winter. Finally, the fourth day corresponds to July 9th, which corresponds to a cloudy day in winter. The configurations assessed for each collector technology considers different solar field areas for the concentrating and non-concentrating technologies, due to the difference in cost for concentrating technologies, to compare the performance of plants with different technologies but achieving a similar LCOH. The solar field areas for the FPC, ETC and PTC technologies are respectively 84,473 m², 84,465 m² and 67,226 m². The

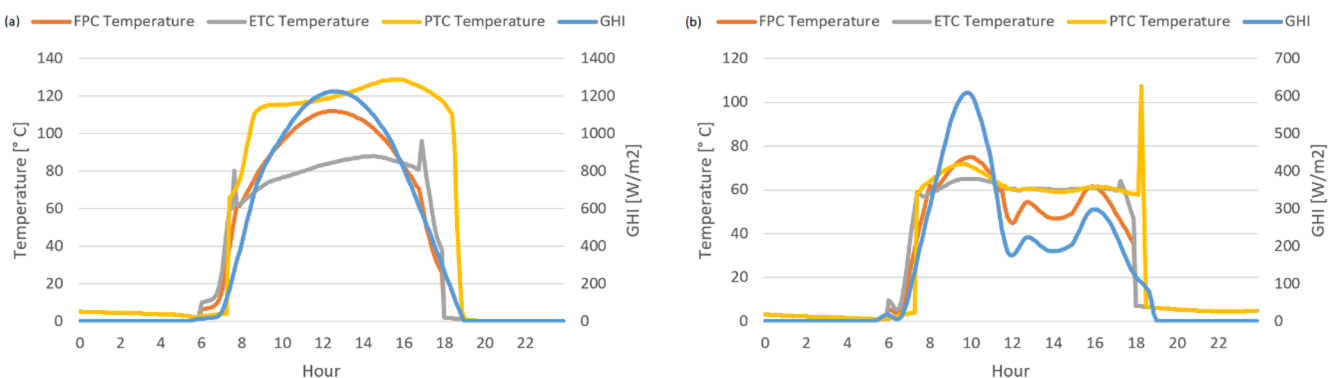


Fig. 14. Outlet temperature from the solar field for each technology in “Los Bronces”, considering two different days. (a) Clear Sky Day in summer (b) Cloudy Day in summer.

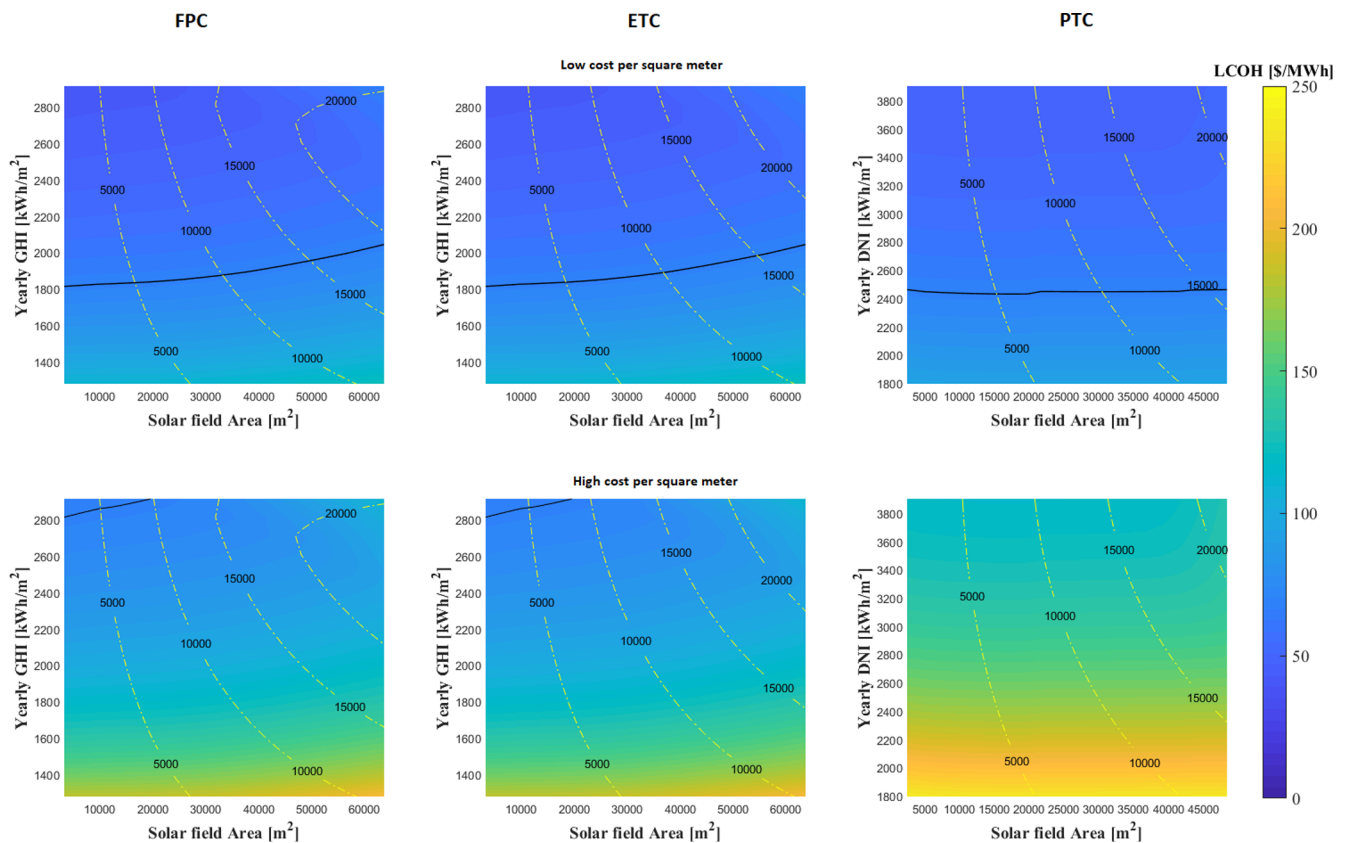


Fig. 15. Parametric analysis. Dashed line: CO_{2e} emissions savings (ton); Solid line: LCOH diesel; color map: LCOH for solar collector.

annual solar fraction of each case is calculated, corresponding to 39.7%, 38.3% and 33.4% for FCP, ETC, and PTC, respectively. These levels of solar fractions values are expected, due to the large number of cloudy sky days observed in the location, which affects the DNI levels, implying a significant decrease on the performance of concentrating technologies, such as PTC.

Figs. 11–13 show the daily profiles of heat demand, fossil fuel consumption, solar heat, and GHI at Los Bronces for each of the three technologies analyzed. For the clear sky case, the three different technologies show a good performance in terms of solar heat delivered to the process, which is even higher than the complement of fossil heat during certain hours of the day. It is worth mentioning that the PTC technology holds the highest performance in clear sky conditions, reaching at least 5 h of solar-only operation, with the fossil heater turned off. On the other hand, for cloudy sky cases, the solar heat delivered by the three technologies is lower than the fossil heat provided to supply the heat demand of the process, and PTC shows a significant decrease in the heat delivered due to its dependence on the availability of DNI. The daily solar fraction of each technology regarding the clear sky days and the cloudy days in summer and winter are shown in Table 10. It is important to note that in Table 10, that in the case of the cloudy day in summer, the solar fraction observed for the PTC technology is higher than the solar fraction for the FPC, mainly due to the storage tank of the PTC have higher remained heat of previous day than FPC. It is also noticeable that during the first hours of the day in Fig. 13(c), where the solar heat has an important contribution to the heat demand even in such early hours when the sun has not come out yet.

On the other hand, it is worth to mention the outlet temperatures from the solar field of each technologie that the systems are capable to reach in summer regarding a clear sky day (9th January) and a cloudy sky day (5th January) in “Los Bronces”. This values represent only the temperature associated to the fluid outlet from the solar field, then this

fluid is stored in the tanks system, allowing to deliver the fluid at the temperature required by the EW process. The outlet temperature is shown in Fig. 14.

3.2. Parametric analysis

A parametric analysis was performed to evaluate the effect on the solar fraction, CO_{2e} emissions reduction and LCOH when varying the collector technology, solar radiation, solar field area and collector cost per square meter. The analysis was carried out using the solar radiation profile for Lomas Bayas mining and the Chilean yearly average of copper production by the EW process (using the previously described data). The solar irradiation profile of Lomas Bayas was selected due to its yearly sum of GHI is nearest to the mean of yearly sum for GHI regarding all the cases studied. This profile is used as a base parameter for this analysis, modifying the solar resource availability, and considered within the parametric analysis amplifying or attenuating this profile. Fig. 15 shows that, when considering the lowest collector cost, the PTC technology results in lower LCOH and the same reduction on CO_{2e} emissions than observed for FPC and ETC with smaller collector area. The tendency for LCOH is inverted when considering higher costs for all technologies. In such case, both non-concentrating technologies present equivalent LCOH and solar fraction values. The continuous line showed in Fig. 15 represents the LCOH of using diesel oil at a market cost of 53.88 USD/MWh_{th} which is a realistic scenario for Chile. LCOH values under that line are those for which solar technologies are competitive with currently used fossil fuel-fired heat supply units.

3.3. Sensitivity analysis

Similarly, a sensitivity analysis of oil and collectors prices was carried out considering the solar resource at Lomas Bayas and the mean heat demand for the EW process in Chile. As mentioned before the solar

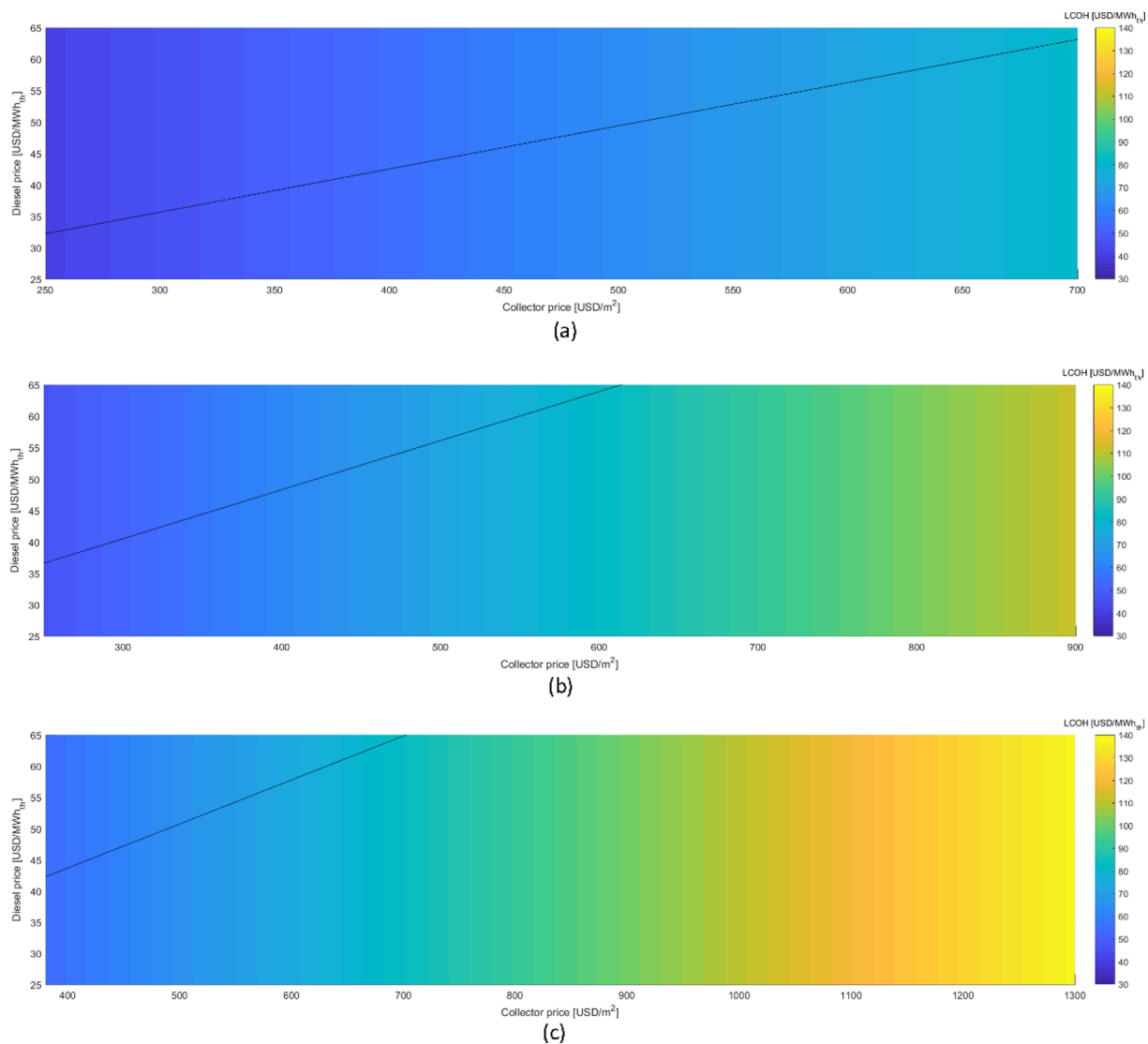


Fig. 16. Sensitivity analysis of collector and diesel price over the LCOH: (a) FPC; (b) ETC; (c) PTC. The solid line shows the limit when it is convenient using of solar energy technologies.

irradiation profile at Lomas Bayas was selected due to its yearly sum of GHI is nearest to the mean of yearly sum for GHI regarding all the cases studied. Three technologies were evaluated with a solar field of approximately 23,000 m², and a storage tank size of 2,530 m³. The results are shown in Fig. 16, considering a range between the lowest and highest oil prices among 2015 and 2019 (ENAP, 2018), and collector cost ranging by technology (aforementioned in Table 5). The results display that the limit values for oil and collector cost displayed as a black line, under which it is more convenient to supply heat by using solar energy technologies that result in lower LCOH levels. High oil prices result in LCOH levels for FPC that can be competitive at 32 USD/MWh_{th}, while ETC and PTC are competitive at 36 USD/MWh_{th} and 43 USD/MWh_{th}, respectively.

4. Conclusions

Copper mining, is the largest energy consumption sector and one of the main contributors to GHG emissions in Chile, mostly utilizing electricity and heat for its extraction and refinement processes. There is a correlation between the location of Chile's largest mining operations and the availability of a high solar resource, which allows proposing schemes for decarbonizing the mining industry by means of solar

energy integration into their production processes. The present quantifies the demand for process heating in large copper mining operations that utilize the EW process, which displays a high consumption of thermal energy in processes at temperatures below 100 °C. The high solar radiation at the different mining operation locations in Chile allows studying the integration of three different solar collectors into the EW process, taking into account the meteorological conditions, and current technology costs for the financial analysis. A solar process heat system model is proposed and validated against publicly available data for two existing solar process heat plants that are currently operating in mining operations located in northern Chile. The system simulations were performed using the TRNSYS software, and the economic model is based on system costs and fossil fuel replacement. The results allow identifying the combination of factors that make the solar heat a competitive alternative to fossil fuels. Avoided CO₂ emissions were also computed based on each configuration of solar fraction results. The three technologies studied are capable of providing the quantity and quality of energy required showing that is feasible to integrate solar thermal systems into the EW process. Fossil heaters are required due to the seasonality of solar resource.

The economic analysis for the three technologies of solar collectors considers scenarios of high, average, and low costs, allowing to

generate a matrix of possible LCOH cases. Analyzing the most favorable economic scenario, which considers the minimum cost for each technology, it is found that the parabolic trough collectors (PTC) results in the lowest LCOH obtained. It is also noted that for this technology the LCOH does not considerably increase with solar field area, and that the best combination of values for LCOH are obtained for large solar field sizes.

When considering the high and average cost scenarios for each technology, the results in both cases indicate that the lowest cost option is the flat plate collector (FPC) technology. In the three cost scenarios, the technology of collectors with evacuated tubes (ETC) displays higher LCOE costs. Given the uncertainties in real capital and operational costs of PTC technologies when installed in northern Chile, a more conservative approach could consider the FPC alternative to the the best option for supplying large quantities of solar heat to the copper refining operations, also considering that FPC technology typically operates at the temperature ranges between 80 and 90 °C that characterize the EW processes.

The benefits that can be obtained by integrating solar heat into EW process are a substantial reduction in CO₂ emissions and positive economic performance. According to the results, solar integration to the EW process is both technically and economically attractive for all the large copper mining operations located in northern.

In future work, other aspects of these systems can be analyzed, including hourly detailed demand functions, storage systems and solar field improving sizing in order to reduce the solar resource variability for supplying continuous solar heat, parametric analysis for diesel costs, the effect of the solar field location relative to the mining pits and refining operations over the O&M costs and lifetime of the plants, and performance due to dust and corrosive chemicals accumulation on the solar field components. Finally, it is important to emphasize that this systems are aligned with the objectives of reduction in CO₂ emissions, and can be very helpful if the policy-making and planning in Chile consider incentives to the implementations of this technologies, such as the incorporation of carbon tax, which can help to improve the economic results of this systems.

Declaration of Competing Interest

The authors declare that they have no known competing financial interests or personal relationships that could have appeared to influence the work reported in this paper.

Acknowledgments

This work was possible thanks to founding Chilean CORFO under the Project 13CEI2-21803, to the National Commission for Scientific and Technological Research grant CONICYT/FONDECYT/1170423, Fraunhofer Chile Research Foundation (FCR) and the collaboration provided by Eduardo A. Salas and Estefanía Quevedo.

References

Abengoa Solar, 2017. Solar plants - Third party plants [WWW Document]. URL www.abengoa.com (accessed 12.20.17).

AChEE, 2018. Capacidades Caloríficas de distintos combustibles y factores de conversión de unidades [WWW Document]. URL <http://www.drto.cl/ACHEE/documentos/recursos/DireccionAnexo2.pdf> (accessed 2.18.19).

Agencia Chilena de Eficiencia Energética, 2011. Capacidades Caloríficas de distintos combustibles y factores de conversión de Unidades.

Aguasol, 2014. Apsol: Manual de diseño de Sistemas Solares Térmicos para la Industria Chilena.

Asociación de generadoras de Chile, 2018. Boletín del mercado eléctrico. Sector generación.

Avaria, P., 2014. Potencia del sol. *Construcción Minera* 5, 40–44.

Avaria, P., 2013. Planta termosolar Pampa Elvira Solar, Minera Gaby. *Construcción Minera* 3, 5.

Banco Central de Chile, 2018. Economía Chilena Diciembre 2018 volumen 21 N°3.

Chandia, E., Zaversky, F., Sallaberry, F., Sanchez, M., 2016. Analysis of the energy

demand of the Chilean mining industry and its coverage with solar thermal technologies. *Int. J. Sustain. Eng.* 9, 240–250. <https://doi.org/10.1080/19397038.2016.1148797>.

Cochilco, 2018. Boletín Mensual de Producción Mundial de Cobre de Mina Anual, Principales Países Diciembre 2018.

Cochilco, 2016. Anuario de estadísticas del cobre y otros minerales 1996 - 2015.

Comisión Nacional de Energía, 2018. Balance nacional de energía 2017 [WWW Document]. URL <http://energiaabierta.cl/visualizaciones/balance-de-energia/> (accessed 8.8.19).

Comité Solar e Innovación Energética, 2019. Formación Comité Solar [WWW Document]. URL <http://www.comitesolar.cl/comite-solar/comite/> (accessed 9.9.19).

Consejo Minero, 2015. Reporte Anual.

Cuevas, F., Murray, C., Platzer, W., Heimsath, A., 2015. Large scale solar plants integration in electro-winning copper recuperation process. *Energy Procedia* 70, 605–614. <https://doi.org/10.1016/j.egypro.2015.02.167>.

Department of Geophysics - University of Chile, 2017. Modelo de Radiación Solar.

Department of Geophysics - University of Chile, Ministry of Energy, 2012. Explorador de energía solar (Solar energy Explorer).

Dietram, O., Maria, M., Tobias, M., Mohamad, E.-N., Elke, Z., 2013. Solar Cooling for Industry and Commerce (SCIC)- Study on the Solar Cooling Potential in Jordan.

E-Llaima, 2017. Pampa Elvira Solar [WWW Document]. URL www.ellaima.cl (accessed 12.20.17).

ellaima, 2015. Pampa Elvira Solar [WWW Document]. URL <https://ellaimasolar.cl/english#engpampaelvira> (accessed 8.8.19).

ENAP, 2018. Tabla de precios de paridad [WWW Document]. URL https://www.enap.cl/pag/66/1295/tabla_de_precios_de_paridad.

Escobar, R.A., Cortés, C., Pino, A., Salgado, M., Pereira, E.B., Martins, F.R., Boland, J., Cardemil, J.M., 2015. Estimating the potential for solar energy utilization in Chile by satellite-derived data and ground station measurements. *Sol. Energy* 121, 139–151. <https://doi.org/10.1016/j.solener.2015.08.034>.

European Copper Institute, 2018. Processes: Copper mining and production [WWW Document]. URL <https://copperalliance.eu/about-copper/copper-and-its-alloys/processes/> (accessed 10.12.19).

Fundación Chile, 2015. Programa Estratégico Nacional en Industria Solar (Road map report - strategic national solar industry program).

Futuro Renovable, 2014. Minería consume termosolar, eólica, fotovoltaica, geotérmica y otras energías renovables en Chile [WWW Document]. URL <https://futurorenovable.cl/mineria-consume-termsolar-eolica-fotovoltaica-geotermica-y-otras-energias-renovables-en-chile/> (accessed 8.8.19).

Gallo, A., Guillaume, M., Portillo, C., Fuentealba, E., 2015. Validation of a solar thermal pilot plant model for copper mining processes. *ISES Sol. World Congr.* 2015, Conf. Proc. 1192–1201. <https://doi.org/10.18086/swc.2015.10.36>.

Gobierno de Chile, 2019. Presidente Piñera presentó plan para cerrar todas las centrales energéticas a carbón para que Chile sea carbono neutral [WWW Document]. URL <https://www.gob.cl/noticias/presidente-piñera-presento-plan-para-cerrar-todas-las-centrales-energeticas-carbon-para-que-chile-sea-carbono-neutral/> (accessed 6.8.19).

Haas, J., Palma-Behnke, R., Valencia, F., Araya, P., Díaz-Ferrán, G., Telsnig, T., Eltrop, L., Díaz, M., Püschel, S., Grandel, M., Román, R., Jiménez-Estévez, G., 2018. Sunset or sunrise? Understanding the barriers and options for the massive deployment of solar technologies in Chile. *Energy Policy* 112, 399–414. <https://doi.org/10.1016/j.enpol.2017.10.001>.

IEA-ETSAP, 2010. Industrial Combustion Boilers, Energy Technology Network.

INE, 2014. Encuesta Nacional Industrial Anual 2014.

Inflation, 2017. Worldwide Inflation Data [WWW Document]. URL <https://es.inflation.eu/tasas-de-inflacion/chile/inflacion-historica/ipc-inflacion-chile-2017.aspx>.

Interempresas, 2013. Minera El Tesoro pone en operación la primera planta termosolar de Sudamérica [WWW Document]. URL <http://www.interempresas.net/Energia/Articulos/104016-Minera-El-Tesoro-pone-en-operacion-la-primer-planta-termsolar-de-Sudamerica.html> (accessed 8.8.19).

International Renewable Energy Agency, 2015. Solar Heat for Industrial Processes Technology Brief.

Kalogirou, S., 2003. The potential of solar industrial process heat applications. *Appl. Energy* 76, 337–361. [https://doi.org/10.1016/S0306-2619\(02\)00176-9](https://doi.org/10.1016/S0306-2619(02)00176-9).

Kalogirou, S.A., 2004. Solar thermal collectors and applications. *Prog. Energy Combust. Sci.* 30, 231–295. <https://doi.org/10.1016/j.pecs.2004.02.001>.

Klein, S.A., et al., 2017. TRNSYS 18: A Transient System Simulation Program.

Louvet, Y., Fischer, S., Furbo, S., Giovanetti, F., Mauthner, F., Mugnier, D., Philippen, D., 2017. LCOH for Solar Thermal Applications.

Mathworks, 2017. MATLAB, the Language of Technical Computing, Version 9.2 (Release R2017a).

MiningPress, 2013. Entra en operación planta Pampa Elvira solar [WWW Document]. URL <http://www.miningpress.com/nota/181038/entra-en-operacion-planta-pampa-elvira-solar->.

Ministerio del Medio Ambiente, 2018. Tercer Informe Bial de Actualización de Chile sobre Cambio Climático 2018.

Ministry of Energy, 2017. Política energética de Chile 2050 (Chile's Energy Policy 2050).

Ministry of Energy, 2016. Balance nacional de energía 2015 (National Energy Balance 2015).

Moreno-Leiva, S., Díaz-Ferrán, G., Haas, J., Telsnig, T., Díaz-Alvarado, F.A., Palma-Behnke, R., Kracht, W., Román, R., Chudinzow, D., Eltrop, L., 2017. Towards solar power supply for copper production in Chile: Assessment of global warming potential using a life-cycle approach. *J. Clean. Prod.* 164, 242–249. <https://doi.org/10.1016/j.jclepro.2017.06.038>.

Murray, C., Platzer, W., Petersen, J., 2017. Potential for solar thermal energy in the heap bioleaching of chalcopyrite in Chilean copper mining. *Miner. Eng.* 100, 75–82. <https://doi.org/10.1016/j.mineng.2016.09.022>.

- Olivares, S.A., 2016. Planta elvira solar - división gabriela mistral. *Energy Thinking Days*.
- Román, R., Hass, J., Díaz, G., 2014. Análisis y diagnóstico de experiencias de plantas solares en Chile en operación y conectadas a la red. Santiago.
- Schlesinger, M.E., King, M.J., Sole, K.C., Davenport, W.G., 2011. Chapter 17 - Electrowinning BT - Extractive Metallurgy of Copper (Fifth Edition). Elsevier, Oxford, pp. 349–372 <https://doi.org/https://doi.org/10.1016/B978-0-08-096789-9.10017-4>.
- Sisó, L., Gavaldà, O., 2009. Components and functional schemes for SAHC in target sectors.
- SNA, 2018. Anuario Estadístico 2018 Aduanas.
- Solar Keymark, 2016. Certificate for HT Heatboost 35/10.
- TÜV Rheinland, 2016. Annex to Solar Keymark Certificate - Summary of EN ISO 9806 : 2013 Test Results for Vitosol 200-TM CP1A 18 tubes.
- U.S. Energy Information Administration, 2016. Carbon Dioxide Emissions Coefficients [WWW Document]. URL https://www.eia.gov/environment/emissions/co2_vol_mass.php.
- Weiss, W., Rommel, M., 2008. Process heat collectors - State of the art within task 33/IV.
- Weiss, W., Spörk-Dür, M., 2018. Solar Heat Worldwide 2018 94.
- Zurita, A., Castillejo-Cuberos, A., García, M., Mata-Torres, C., Simsek, Y., García, R., Antonanzas-Torres, F., Escobar, R.A., 2018. State of the art and future prospects for solar PV development in Chile. *Renew. Sustain. Energy Rev.* 92, 701–727. <https://doi.org/10.1016/j.rser.2018.04.096>.